RESEARCH ARTICLE

GAS SEPARATION PERFORMANCE OF POLYMERIC MEMBRANES FOR FLUE GAS CAPTURE AND HELIUM SEPARATION

[1,2,*]**Neha Bighane**, [1]**Sridhar S.**, [2]**Srinivasan Madapusi**, [2]**Suresh Bhargava** and [1]**Ramanuj Narayan**

[1]CSIR-Indian Institute of Chemical Technology, Uppal Road, Tarnaka, Hyderabad 500007, India
[2]School of Engineering, the Royal Melbourne Institute of Technology, GPO box 2476,Melbourne, VIC 3001, Australia

ARTICLE INFO

ABSTRACT

Coal combustion power plants produce tons of by-product flue gas emissions. Flue gas mainly comprises a mixture of carbon dioxide and nitrogen. CO2 is a greenhouse gas and its emissions contribute to global warming in the atmosphere. It is important to develop technologies to separate and capture CO2 before it is emitted into the atmosphere. Membranes are robust materials that provide selective permeation of one gas from a mixture under a partial pressure gradient. The separated gas streams can be utilized for various purposes or sequestered. In this paper, gas separation performance of dense films of polyethersulfone, polysulfone, novel pure Torlon®AI-10 polyamide-imide membrane and four novel mixed matrix membranes of Torlon with Zif-8 nanoparticles is presented. In pure Torlon membranes, the observed pure gas CO2/N2 selectivity is 40 and He/N2 selectivity is 97 at 60psia feed pressure at 25°C. In Torlon-Zif8(10%) mixed matrix membranes, He/N2 selectivity is 192 at 100psia. In mixed gas experiments, we obtained 99.8% pure CO2 in permeate from Torlon-Zif8(20%) mixed matrix membrane dense films. Material characterization studies include DMTA, DSC, TGA, FTIR, SEM, XRD and UTM. The developed membranes are suitable for flue gas separation. The membranes can also lower cost and improve energy efficiency in helium extraction process.

Citation: Neha Bighane, Sridhar S., Srinivasan Madapusi, Suresh Bhargava and Ramanuj Narayan, **2018.** "Gas separation performance of polymeric membranes for flue gas capture and helium separation", *Asian Journal of Science and Technology*, 09, (10), 8811-8832.

INTRODUCTION

Gas separation membranes are robust materials that provide selective permeation of one gas from a mixture under a partial pressure gradient. Owing to their microscopic structure and properties, membranes allow preferential permeation of one gas from a mixture. Upstream pressure of feed gas on membrane is high while downstream pressure is low. Membranes based separations work on the principle of a pressure driving force and hence provide higher energy efficiency, low cost, simplicity in operation, compactness and portability. Membrane technology can be combined with existing steps in industrial production to improve overall efficiency of a process and increase throughput of the desired product. This paper describes performance of new membranes for flue gas capture and helium separation. Industrial gas emissions leave greenhouse gases in the Earth's atmosphere causing global warming. Greenhouse gases entrap heat in the atmosphere and include CO_2, O_3, CH_4, H_2O, N_2O and fluorinated gases. Carbon dioxide emissions of countries have increased over the past years. The CO_2 emissions of the world were 35,688,794 ktons in 2014 (EDGAR (2018). CO_2 enters the atmosphere from burning of fossil fuels (coal, natural gas and oil for electricity generation), solid waste, trees, wood products, vehicles and from certain chemical reactions like manufacture of cement and steel. CO_2 is removed from the atmosphere when it is absorbed by plants as part of the biological carbon cycle. Industrial flue gas contains 70% nitrogen, 11-20% carbon dioxide,1.5-4% oxygen, 3-7% water vapor, 100-500ppm nitrous oxides and 300-2000ppm of sulphur oxides depending on the composition of the fuel burnt (Powell *et al.*, 2006). In a pulverized coal power plant, fuel is burned in air to produce heat energy that heats water to steam that drives a turbine/generator to produce electricity and by-product flue gas is produced that is vented into the atmosphere or can be captured post-combustion. Flue gas from cement plants contains 25%CO_2, steel plants contain 25%CO_2 and biomass boiler contains 14%CO_2 (Rochelle (2009). The 2007 Stern report suggested a global reduction in CO_2 emissions would cost 1% of the world GDP whereas a 1.1 to 6.4°C rise in temperature could cost as much as 20% to repair (6, Maslin (2004). Atmospheric CO_2 was at 379ppm in 2004 and has reached 403ppm in 2017 (CO_2earth (2017).

Corresponding author: [1,2]**Neha Bighane,** [2]**Srinivasan Madapusi,**
1CSIR-Indian Institute of Chemical Technology, Uppal Road, Tarnaka, Hyderabad 500007, India
2School of Engineering, the Royal Melbourne Institute of Technology, GPO box 2476,Melbourne, VIC 3001, Australia

The temperature of the Earth is determined by the balance of energy between that input by the Sun and that reflected back into space by the Earth. The energy received from the Sun is in the form of shortwave radiation and ultraviolet. On an average, about two-third of the incoming solar radiation is absorbed by the atmosphere, land and oceans. The Earth's surface becomes warm and as a result emits long wave radiation that warms the atmosphere. Greenhouse gases create a natural greenhouse or blanket effect. It is predicted that a 1-4°C rise in global temperatures can lead to collapse of the North Atlantic circulation. Global warming will affect the severity of floods, droughts, heat waves and storms (Houghtan, 2001; McCarthy, 2001; Pacala *et al.,* 2004). Global warming can be solved by building international agreements to reduce anthropogenic global greenhouse gas emissions. In 1992, the UNFCCC recognized climate change as a global challenge. In 1997, the Kyoto protocol gathered around 180 countries to sign the reduction in emissions global warming pact. Convened by the UN, the 2015 Paris Agreement, the latest international climate treaty, has aimed to keep global temperature rise less than 2°C and to maintain atmospheric CO_2 below 450ppm in near future (time.com (2018). There are about 3250 coal power plants installed throughout the world (1627GW total capacity). A typical pulverized coal power plant produces 300-500MW of electrical energy and releases 6-9 ton of CO_2/min (Lively *et al.,* 2009). Volumetric flow rate of flue gas is about 500m³/sec (Merkel *et al.,* 2010). Instead of venting flue gas into the atmosphere, it can be sent to a membrane unit where it will get separated into a useful CO_2 permeate stream and a N_2 retentate stream that can be used or safely vented. Membranes are materials that facilitate separation in industrial chemical processes based on partial pressure driving force. The advantages of using membranes are that the cost of thermal energy in conventional separation processes such as amine absorption for CO_2 capture or distillation for He separation is reduced, the efficiency of the separation process increases and the overall cost of a production process gets altered to a lower value. For flue gas purification, gas separation membranes need to achieve moderate CO_2 permeability and high CO_2/N_2 selectivity. Figure 1 is proposed schematic diagram of processing power plant off gas by a CO_2 selective membrane unit.
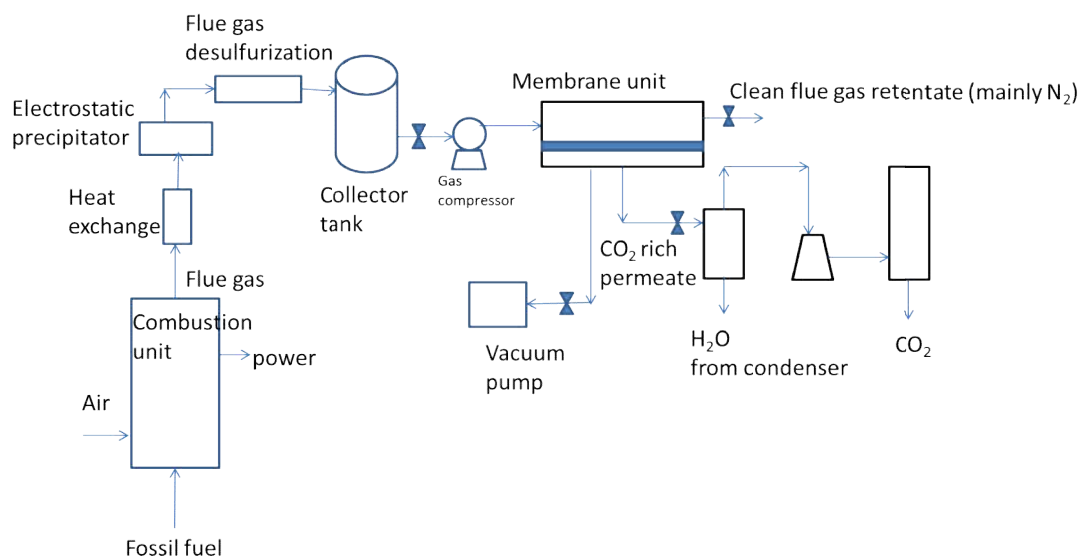

Figure 1. Proposed schematic diagram for processing power plant off gas by a CO_2 selective membrane unit

In conventional coal power plants, air reacts with coal at very high temperatures of about 1200°C at 1atm to generate power and by-product flue gas. The generated flue gas is at high pressure and high temperature. This flue gas is passed through a heat exchanger for cooling, electrostatic precipitator for particulate removal and flue gas desulfurization (limestone slurry) to meet emission standards. At this point, flue gas is at 50°C and 1 atm (Merkel *et al.,* 2010). This hot air keeps flowing out through the chimney by natural draft or by a draft fan. Instead of venting into the atmosphere, the flue gas can be compressed and sent to a membrane unit. Any pressure between 30-75psia can be set as the 'gas compressor' outlet pressure or feed flue gas to membrane unit. On a semi-continuous basis, feed gas would be fed to the membrane chamber. Carbon dioxide, water vapor and small traces of oxygen would permeate through the membrane due to pressure difference while nitrogen would remain in the retentate. The permeate can be collected in the downstream collector at atmospheric pressure (14.7psia) or under vacuum, as depicted in figure 1. An automatic or manual valve in the retentate line can be used to increase residence time of feed gas in the membrane unit and would open to vent retentate when the concentration of CO_2 in the upstream membrane chamber becomes lower than 2%. Then, fresh feed would enter the membrane unit. The collected permeate CO_2 can be used as a gas for various applications or it can be compressed into supercritical liquid to use for enhanced oil recovery. After every 24 hours, the membranes will be de-gassed for 4 hours by a vacuum pump (Edwards company). Helium gas is mostly extracted from a four-stage cryogenic fractional distillation of natural gas. The boiling point of helium is -269°C. The global reserves of helium are ~41 billion cubic meters; most of them lie in Qatar, Algeria, the USA (New Mexico, Texas), Canada, Poland, Australia and Russia. Helium concentration in natural gas wells lies in the range 0.05-4mol% and well-head pressure varies from 360-1450psia (Scholes *et al.,* 2016). After acid gas removal, mercury removal and dehydration, in the first stage, methane is liquefied using low temperature (< -161°C) and high pressure to produce Liquefied Natural Gas (LNG) and off-gas. The off-gas is sent to second stage nitrogen rejection unit (NRU) in which very low temperatures (-140 to -180°C) in distillation columns cause residual methane to liquefy. The liquid is recycled to the first stage while the off-gas containing low mole% helium in remainder nitrogen (boiling point -195°C), oxygen and hydrogen is sent to third stage (16, Scholes et.al.(2016). In third stage, helium recovery is achieved by cryogenic distillation to liquefy

nitrogen/oxygen and get 50-70% crude helium. In fourth stage, helium upgrading is achieved through cryogenic condensation of residual gases, catalyzed oxidation of hydrogen and pressure swing adsorption to remove trace amounts of H_2 and N_2 and get 90% helium. Activated charcoal is used in the final purification step. In another final purification step, all of the helium produced is liquefied in a cryogenic process (< -246°C) to separate neon impurity to obtain 99.9% pure helium. Use of membranes to separate helium from nitrogen and methane can provide energy and cost savings in this industrial process. If the off-gas from NRU is high pressure, it can be expanded to lower pressure (30-75psia) or the off-gas from NRU can be compressed to 30-75psia and fed to a membrane unit to achieve helium separation by membranes. Helium will permeate through the membrane due to pressure difference (downstream at atmospheric 14.7psia or vacuum) while nitrogen will remain in the retentate. Membranes will be able to concentrate 50-98% Helium in permeate, as depicted in figure 2. This will be followed by final purification and liquefication.
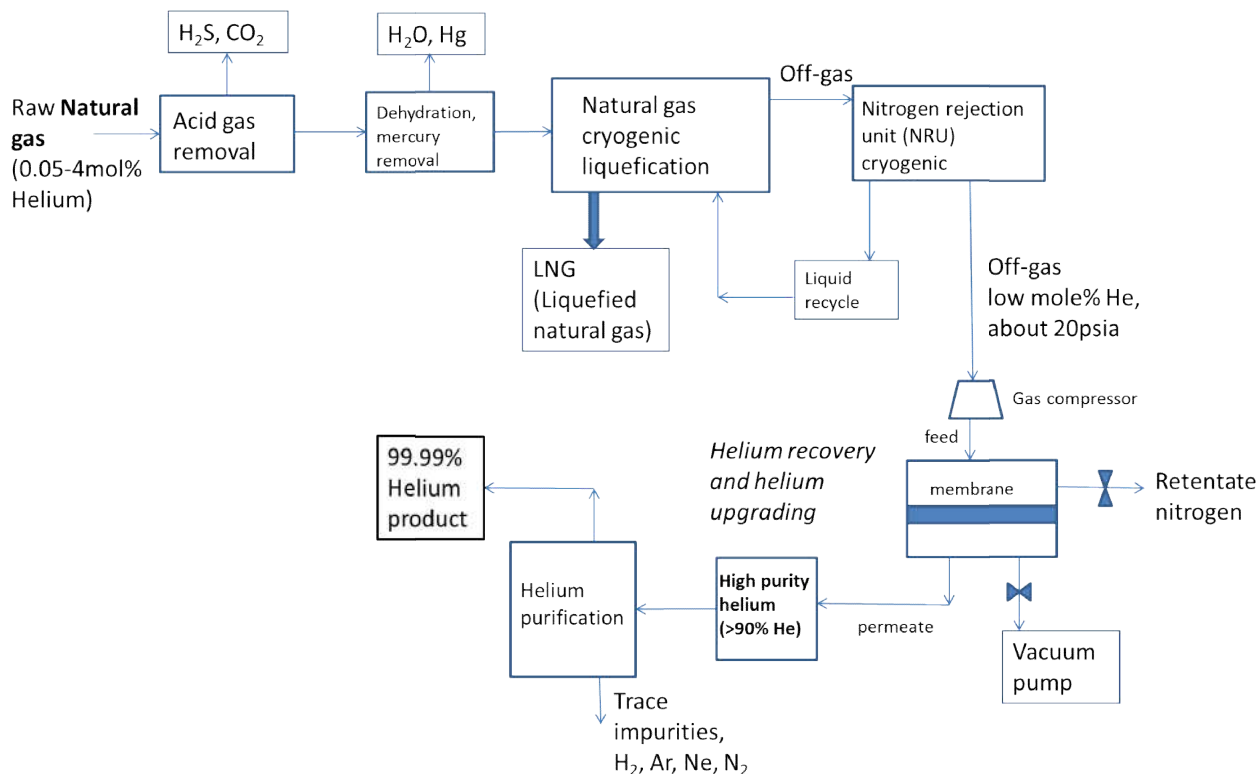

Figure 2. Proposed schematic diagram for helium separation by membranes, in cryogenic extraction from natural gas

The objective of this paper is to study experimental data on gas permeability and selectivity for polyethersulfone, polysulfone, Torlon AI-10 polymeric membranes and four Torlon-Zif8 mixed matrix membrane dense films, for the two mentioned applications.

Theory

Gas permeation is a combination of adsorption and diffusion in membranes. The separation ability of membranes is attributed to their intrinsic properties i.e. chemical structure in case of a polymer, pore size in case of zeolites, interfacial adhesion in case of mixed matrix or hybrid membranes and mechanical strength in all cases. In polymeric membranes, the gas transport is governed by solution-diffusion. In a mixed matrix membranes, microporous nanoparticles are uniformly dispersed in a polymer matrix to combine the advantages of ease of fabrication and mechanical strength of polymers with size based exclusion property of nanoparticles. Commercially available polymers that provide good gas separation are Ultem®, Matrimid® and Torlon®4000T. Gas separation membranes can be fabricated in symmetric dense film form by solution casting and heat-drying in vacuum method. The same polymer can also be developed into a hollow fiber configuration by volatile solvent aided 'dry-jet wet-quench' phase inversion method in water to obtain an asymmetric membrane with a thin dense selective skin layer on the outer surface and a microporous substructure (Lively *et al.*, 2012; Kosuri *et al.*, 2008). Dense membrane films tend to be significantly thicker than the selective layer of asymmetric hollow fiber membranes. But the dense film membrane and the dense selective skin layer on the asymmetric hollow fiber of the same polymeric material provide the same gas separation selectivity. This fact is also valid for mixed matrix membranes (Lively *et al.*, 2012). A gas separation membrane is a selective barrier between two gaseous phases. Owing to its microscopic structure and properties, it allows preferential passage of one gas from a mixture. A membrane is characterized by its permeability (productivity) and selectivity (efficiency). Permeability of a gas through a membrane is defined as the flux normalized by the pressure driving force.

$$P_i = D_i \cdot S_i = \frac{(\text{Flux})_i}{\Delta p_i / l} \qquad (1)$$

Permeability is related to the product of the diffusivity D_i (dependent on molecular size of gas relative to pores in membrane) and the adsorption coefficient S_i (dependent on adsorption/condensability of gas in membrane) of the penetrant gas molecule in the membrane. This is called the solution-diffusion model. P_i is the permeability of gas i, through the membrane, Δp_i is the partial pressure difference of gas i across the thickness of the membrane and l is the thickness of the membrane. The commonly used unit of permeability is Barrer.

$$1\,\text{Barrer} = 10^{-10}\,\frac{\text{cm}^3(\text{STP})\cdot\text{cm}}{\text{cm}^2\cdot\text{sec}\cdot\text{cm Hg}} = 3.348\times10^{-16}\,\frac{mol.m}{m^2.s.Pa} \qquad (2)$$

The ratio of the permeabilites of pure gases at the same pressure and temperature is defined as ideal selectivity α. For a mixed gas feed, the separation factor β of a membrane is the ratio of the mole fractions of gas i to gas j in permeate divided by the ratio of mole fractions in the upstream.

$$\text{Selectivity } \alpha = \frac{P_i}{P_j} \qquad (3a)$$

$$\text{Separation factor } \beta = \frac{\left(\frac{yi}{yj}\right)permeate}{\left(\frac{xi}{xj}\right)feed} \qquad (3b)$$

Hollow fiber membrane fabrication systems have high production rates due to multi-filament spinning capabilities and offer high module surface area-to-volume ratios approaching $10,000\,\text{m}^2/\text{m}^3$ device. In an asymmetric membrane, permeance is measured in GPU because it is difficult to determine the thickness of the separating layer.

$$1\text{GPU (Gas permeation units)} = \frac{10^{-6}\,\text{cm}^3(\text{STP})}{\text{cm}^2.\ \text{sec.cm-Hg}} \qquad (4)$$

Table 1. Physical parameters of relevant gas molecules ($1\text{Å}=10^{-8}\text{cm}=0.1\text{nm}$)

Gas	Kinetic diameter (Å)	Critical temperature (K)	Electric Moment
Helium	2.6	5.15	0
Water vapor	2.65	647.14	Dipole: 1.8546×10^{-18} esu.cm
Carbon dioxide	3.3	304.15	Quadrupole: $- 4.3 \times 10^{-26}\text{erg}^{1/2}\text{cm}^{5/2}$ [22]
Oxygen	3.46	154.6	Quadrupole: $-0.4 \times 10^{-26}\ \text{erg}^{1/2}\text{cm}^{5/2}$
Nitrogen	3.64	126.15	Quadrupole: $-1.52 \times 10^{-26}\ \text{erg}^{1/2}\text{cm}^{5/2}$
Methane	3.8	190.45	0

CO_2 is smaller and more adsorbing than N_2; therefore, CO_2 would permeate faster through a membrane. Similarly, He is smaller than N_2 and He would permeate faster than N_2 through a membrane. According to the solution-diffusion theory, three steps can be used to describe the mass transport of species within the membrane film: (1) adsorption of species on the feed side of the membrane, (2) diffusion of components through the membrane and (3) desorption from the permeate side of the membrane. The rate at which gases permeate through a polymeric membrane primarily depends on the fractional free volume in the membrane and chain packing of polymeric chains. Presence of bulky groups provides high fractional free volume leading to high CO_2 permeability and closely packed rigid chains provide high selectivity.

Literature Survey

Use of gas separation membranes for flue gas capture is in R&D stage. Some pilot plant tests have been reported. This section comprises a literature survey of membranes for CO_2/N_2 separation. Table 2.1 lists membranes of different types, their corresponding permeability and CO_2/N_2 selectivity values. There is limited literature on helium separation. Table 2.2 lists membranes of different types, their corresponding permeability and He/N_2 selectivity values.

Experimental

Membrane fabrication: In this section, fabrication of dense membrane films of pure glassy polymers Torlon polyamide-imide, polyethersulfone, polysulfone and four mixed matrix membranes of Torlon with 5%,10%,15% or 20% ZIF-8 nanoparticles is described. Solution casting and complete evaporation of solvent technique was employed for forming dense membrane films. The pure polymeric membranes are nonporous membranes. The mixed matrix membranes are combination of microporous nanoparticles in nonporous polymeric membrane. Polymer Torlon® AI-10 polyamide-imide and polymer Veradel® 3000P polyethersulfone were purchased from Solvay advanced polymers, India. Polymer polysulfone (Mw=35,000, Mn=16,000), solvent NMP n-methyl 2-pyrrolidone (99%, anhydrous, 328634_1L) and Basolite® Z1200 ZIF-8 nanoparticles were purchased from Sigma-Aldrich, India (Zif8 powder: density 0.35gm/cm³, BET surface area 1810m²/gm, pore volume 0.63cm³/gm). Torlon 4000T is a random co-polymer prepared by reacting TMACl (trimellitic anhydride acid chloride) with two diamines:

Table 2.1. Literature survey of membranes for carbon dioxide-nitrogen separation

S. No.	Membrane material	Temperature (°C)	Type of membrane	CO_2 permeability (Barrer)	N_2 permeability (Barrer)	Selectivity CO_2/N_2	Reference
1	17 vol% ZIF-8/ Ultem® hybrid hollow fiber	35	Mixed matrix membrane	26GPU	0.72GPU	36	(Dai *et al.,* 2012)
2	Torlon® 4000T polyamide-imide	35	Glassy polymer	0.47	0.014	33	(Kosuri *et al.,* 2008; Kosuri, 2009)
3	20wt%Zif-8/6FDA-DAM/DABA polyimide	35	Mixed matrix membrane	550	28.95	19	(Lively *et al.,* 2012)
4	Poly(methyl acrylate)	35	Rubbery polymer	6.67	0.187	35.67	(Koros *et al.,* 1988)
5	Crosslinked polyethylene glycol-methyl ether acrylate	35	Rubbery polymer	66	1.6	41	(Scholes *et al.,* 2012)
6	Polaris® membrane by Membrane Technology and Research, Inc.	30	Supported rubbery polymer	1000GPU	20GPU	50	(Merkel *et al.,* 2012)
7	6FDA-BPDA/DAM coated with PDMS	-50°C	Glassy polymer	500GPU	2.3GPU	214	(Liu *et al.,* 2016)
		35	Glassy polymer	498GPU	21.1GPU	23	
8	Polyethylene oxide polymer	35	Polymer with enhanced CO_2 solubility	12Barrer	0.25Barrer	48	(Liu *et al.,* 2016)
9	1,6-hexanediamine cross linked polyurethane	35	Rubbery polymer thin film on alumina support	76.9	2.6	29.6	(Ishfahani *et al.,* 2016)
10	Silica-titania	35	Inorganic membrane	380.55	13.67	27.84	(Neha, 2017; Neha, 2013)

Table 2.2. Literature survey of membranes for helium-nitrogen separation (permeability in Barrer)

S.No.	Membrane	T (°C)	Membrane Type	Helium permeability	Nitrogen permeability	He/N_2 selectivity	Ref.
1	Polyamide Nylon 6	25	Glassy polymer	2.43	0.0246	98.8	(Pienemann, 1986)
2	Polyethylene terephthalate Mylar	25	Amorphous polymer	2.967	0.0144	206	(Pienemann, 1986)
3	Polyvinyl fluoride	25	Glassy polymer	0.97	0.0042	231	(Pienemann, 1986)
4	Polyvinylidene chloride	25	Rubbery polymer	0.066	0.00018	366	(Pienemann(1986)
5	Polyetherimide Ultem®	25	Asymmetric glassy polymer film	-	-	234	(Pienemann (1986)
6	Torlon® 4000T	35	Glassy polymer	4.4	0.014	310	(Kosuri *et al.,* 2008)
7	PIM-1fibers	35	Polymer of intrinsic microporosity	190GPU	13GPU	14.6	(Jue *et al.,* 2017)
8	Matrimid fibers	35	Glassy polymer	243GPU	2.7GPU	90	(Jue *et al.,* 2017)
9	Carbon membrane derived from 6FDA-BPDA/DAM	35	Microporous carbon membrane	2530Barrer	204Barrer	12.4	(Kiyono *et al.,* 2010)
10	Silica derived from PDMS	35	Microporous inorganic membrane	735.7	79.6	9.2	(Bighane *et al.,* 2011; Bighane, 2012)
11	Ni doped Silica	300	Supported Sol-gel microporous membrane	2198GPU	1.51GPU	1450	(Kanezashi, 2006)

ODA (4, 4'-oxydianiline) and m-PDA (m-phenylenediamine). It has glass transition temperature of about 270°C and can withstand 1100psia CO_2 withreversible swelling (Kosuri *et al.,* 2008; Kosuri 2009). Torlon AI-10 is a polymer prepared by reacting trimellitic anhydride acid chloride with 4,4'-methylene dianiline. Polyamic acid intermediate is formed that gets converted into imide groups upon thermal or chemical imidization. In this work, we have used only Torlon AI-10. Its glass transition temperature was measured to be 175°C and it can withstand 300 psia of helium with reversible swelling. A special feature of Torlon® polymeric membranes is inter-chain hydrogen bonding between hydrogen of amide group and carbonyl oxygen between neighboring chains that keeps the chain packing very rigid. The viscosity of the Torlon AI-10 solution in NMP is a parameter to define the molecular weight and it is 1.00Pa.s (23°C, 25% in NMP, ±300mPa.s). Mixed matrix membranes combine the ease of processing and high mechanical strength of polymers with the size-based exclusion property and high permeability of microporous nanoparticles.

Fabrication of pure Torlon (or polyethersulfone or polysulfone) membrane: A solution of the polymer 4gm Torlon (18weight%) in NMP 18gm (n-methyl 2-pyrrolidone) was prepared by magnetic stirring for 6 hours and let stand at room temperature for 18 hours. The clear brown solution was poured onto a clean glass plate and drawn cast into a film with a graduated glass rod, which is called solution casting. The glass plate with the film was placed in a convection oven (Memmert UF110) at 90°C for 24 hours. Complete evaporation of solvent dried the film. The film was peeled off the glass plate. Unsupported defect free film was obtained. The polymeric membrane is flexible and strong. The area of the yellow transparent film was 320cm² for 0.09mm thickness (400cm² for 0.07mm).

Fabrication of Torlon with 5% or 10% ZIF-8 mixed matrix membranes: For preparing 10% Zif8 in Torlon, a solution of the polymer Torlon 4gm (19weight%) in NMP 17gm (n-methyl 2-pyrrolidone) was prepared in a glass jar by magnetic stirring for 6 hours and let stand at room temperature for 18 hours. A solution of 0.5gm of ZIF8 in 4gm NMP was prepared in a glass vial and sonicated for 20 minutes two times over 24 hours. Sonication provided a homogeneous milky white dispersion of ZIF8 particles in NMP. Soon after second sonication, the ZIF8 solution was mixed with the polymer solution by stirring with a spatula for 2 minutes and allowed to stand for 30minutes for air bubbles to disappear. The mixed solution was poured onto a clean level glass plate and drawn cast into a film with a graduated glass rod. Soon after casting, the plate was placed in a convection oven and left at 90°C for 24 hours. Complete evaporation of solvent dried the membrane. Unsupported defect free film was carefully peeled off the glass plate. This area of this yellow semi-transparent film was about 380cm² (0.07mm thickness). The novel mixed matrix membrane film is flexible, strong and has 11% Zif8 in Torlon polymer. (Optionally, the film can be allowed to dry at room temperature for 24 hours before drying in oven).

Figure 3a. Photograph of yellow Torlon AI-10 dense membrane film

Figure 3b. Photograph of Torlon-Zif8(10%) mixed matrix membrane dense film

Figure 3c. Photographs of Torlon-Zif8(20%) mixed matrix dense membrane films

Fabrication of Torlon with 15% or 20% ZIF-8 mixed matrix membranes: For preparing 20% Zif8 in Torlon, a solution of the polymer Torlon 4gm (19weight%) in NMP 17gm (n-methyl 2-pyrrolidone) was prepared in a glass jar by magnetic stirring for 6 hours and let stand at room temperature for 18 hours. A solution of 1gm of ZIF8 in 6gm NMP was prepared in a glass vial and sonicated for 20 minutes two times over 24 hours. Sonication provided a homogeneous milky white dispersion of ZIF8 particles in NMP. Soon after second sonication, the ZIF8 solution was mixed with the polymer solution by stirring with a spatula for 2 minutes and allowed to stand for 30minutes for air bubbles to disappear. The mixed solution was poured onto a clean level glass plate and drawn cast into a film with a graduated glass rod. Then, the plate with the film was placed in a convection oven and left at 90°C (60% fan, 40% flap in oven). After about 2 hours, the film gets peeled off the glass plate and it was left in the oven at 90°C for 24 hours. Complete evaporation of solvent dried the membrane. Unsupported defect free film was obtained. The novel mixed matrix film is flexible, strong and has 20% Zif8 in Torlon polymer. The area of the yellow opaque film was about 260cm^2 and it is curled from edges with 0.08mm thickness. For Torlon-Zif8(15%) membranes, solution of 3gm Torlon in 15gm NMP was

mixed with solution of 0.55gm Zif8 in 4gm NMP, cast and dried the film for 3 days at room temperature, 5 hours at 90°C, peeled off the film and left to dry at 90°C for 24 hours. These membrane films experience 'drying stresses' in the oven.

Fabrication of hollow fibers: Novel asymmetric hollow fibers of pure Torlon AI-10 were prepared. A 21wt% solution of Torlon polymer in mixed solvent 6:2 NMP and THF (tetrahydrofuran) was allowed to dissolve for 5days at 25°C with stirring, in a capped glass jar. The homogeneous brown dope solution was extruded through an annular spinneret with water as the bore fluid. Volatile solvent THF escaped in an air gap of 22cm to form a 'dense skin layer' on the outer surface of the hollow fiber. The hollow fiber got quenched in a non-solvent water bath in which 'phase inversion' of polymer and rapid exchange of solvent and non-solvent lead to formation of a micro/mesoporous substructure of the hollow fiber membrane. The fibers were soaked in de-mineralized water for 5 days with daily exchange of water to remove residual solvent and increase mechanical strength. Then, the fibers were allowed to dry at 25°C for 2 days and then dried at 70°C for 2 hours. The hollow fibers are flexible and strong. SEM image of the cross-section of hollow fiber membrane showed a defect-free dense outer surface (membrane layer) and a microporous substructure. At some places, the substructure had some macrovoids. Formation of macrovoids can be avoided by increasing the polymer concentration in the dope solution to about 34% (Kosuri *et al.,* 2008).
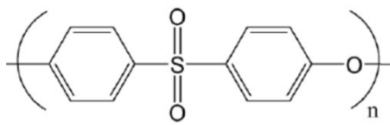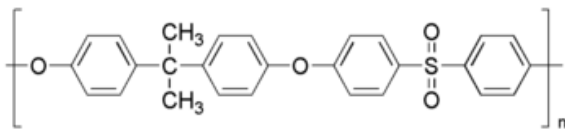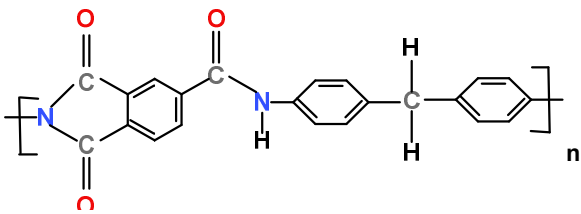
Material characterization

The fabricated membrane films were investigated for density, glass transition temperature, various chemical bonds, micromorphology and strength. Differential scanning calorimetry (DSC) was performed on pure polymer membrane films using DSC-Q100 machine. A plot of heat flow vs. temperature was obtained. An endothermic (downward) shift in baseline indicated the glass transition temperature of the polymer. Tg is the temperature which a polymer transitions from glassy state to rubbery state. Differential mechanical thermal analysis (DMTA, DMA Q800 TA instruments) was performed on Torlon, Torlon-Zif8(10%) and Torlon-Zif8(20%) membrane films and a step transition in storage modulus indicated the glass transition temperatures.

The weight of a measurable area and thickness of pure polymer membrane was obtained and density was calculated as in equation 5.

$$\rho = m/V = m/(A \times \delta) \tag{5}$$

Molecular structure of repeat unit of studied polymers, density and Tg results are in Table 3.

Table 3. Polymer name, molecular structure of repeat unit, density and glass transition temperature as measured from DSC

Polymer name	Molecular structure	Density (gm/cc)	Glass transition temperature(°C)
Polyethersulfone		0.9437	155.54
Polysulfone		0.9893	98.61
Torlon® AI 10 polyamide-imide		1.1969	175.12

From DMTA (Figure 4a), we observed glass transition temperatures as Tg=176.5°C for pure Torlon AI-10, Tg= 181.4°C for Torlon-Zif8(10%) and Tg= 172.4°C for Torlon-Zif8(20%). In DSC on pure Torlon AI-10 polyamide-imide film, we observed disruption of hydrogen bonding among chains at 120°C, glass transition at 175°C, short rubbery region plateau from 175-190°C and decomposition at higher temperatures. Thermogravimetric analysis (TA TGA-Q500 machine, N_2 purge) on Torlon AI-10 film revealed a first step 3.3% weight loss up to 175°C (residual solvent or moisture) and second step 18% total weight loss at 350°C (Figure 4 b). This confirmed that our membrane films were completely dry after fabrication and that polymer decomposition begins at 175°C. The same TGA was observed for Torlon-Zif8(15%) mixed matrix film. Fourier Transform infrared spectroscopy was performed on pure polymer membrane films using Perkin Elmer Spectrum 100 machine. FTIR is a material characterization technique in which exposure of a sample to IR beam yields characteristics peaks of various chemical bonds present in the sample. Chemical bonds corresponding to each peak in FTIR results for Torlon are described in Figure 5. Torlon has high Tg of 175°C. From its FTIR (Figure 5), we observe presence of amide (3482, 3296, 1667 cm^{-1}), imide (1778,1715 cm^{-1}) and aromatic groups (3000, 854,723cm^{-1}) in Torlon structure. Hydrogen bonded N-H stretch occurs at 3353cm^{-1}.
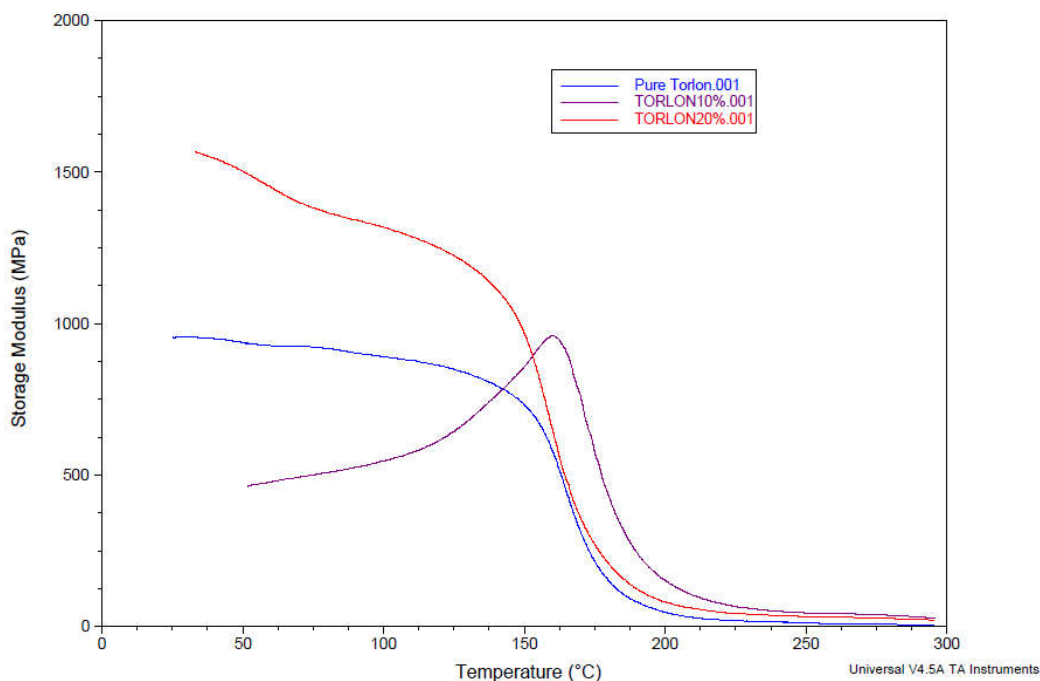
Figure 4a. DMTA on Torlon(blue), Torlon-Zif8(10%)(purple) and Torlon-Zif8(20%)(red) films
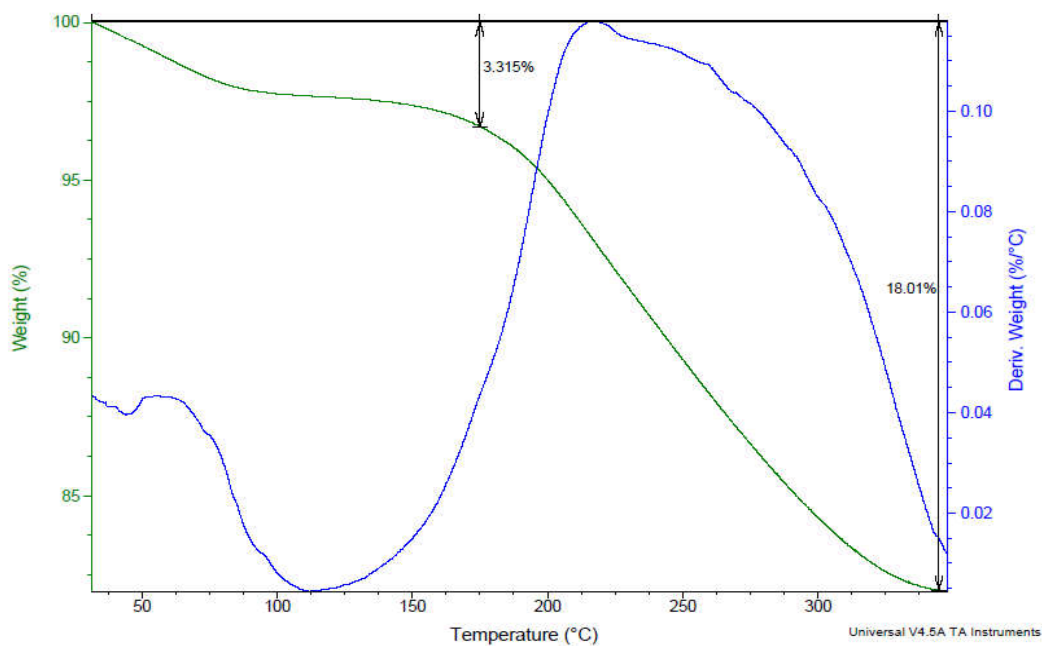

Figure 4b. Thermogravimetric analysis of Torlon AI-10 polyamide-imide dense film

This structure renders Torlon low fractional free volume and closely packed chains that results in good separation ability of the membrane. Scanning Electron Microscopy (Hitachi S-3000N machine) and Field Emission-Scanning Electron Microscopy (JEOL 7610F machine) was performed on mixed matrix membrane films of Torlon with ZIF8 nanoparticles to observe micromorphology. The images were taken in high vacuum. Figure 6a) is FE-SEM of pure Torlon dense membrane film. At magnification of 2000 and pixel size 49.6, the SEM images obtained in figures 6 b),c)d) show well-dispersed particles of ZIF8 embedded in polymer Torlon. From images obtained at higher magnification 10000 and pixel size 9.9, figures 6 e),f) show good interfacial adhesion between particle and polymer. There are no defects and no gaps at the interface between single Zif8 particle and polymer Torlon in the membrane. Perfect adhesion and compatibility is seen. EDS elemental detection spectra on pure Torlon gave 69.6%C, 20.1% O and 10.3%N. EDS elemental detection spectra on Torlon-Zif8(15%) mixed matrix membrane gave 65.1%C, 20.2% O,12.6%N and 2.1%Zinc. Tensile strength of the Torlon based membranes was measured on DAK system Inc, Series 7200 universal testing machine. Results are in Table 4. X-ray diffraction was performed on Zif-8 powder and Torlon with 15% Zif8 mixed matrix film. XRD or X-ray crystallography is a technique in which incident X-rays are scattered by atoms arranged in a crystal lattice of the material. The interaction of the incident rays with the sample produces constructive interference (and a diffracted ray) when conditions satisfy Bragg's Law ($n\lambda = 2d \sin \theta$). This law relates the wavelength of electromagnetic radiation to the diffraction angle and the lattice spacing in a crystalline sample. These diffracted X-rays are then detected, processed and counted. All possible diffraction directions of the lattice are obtained. XRD results are in figures 7a and 7b. From figure 7a) we observe crystalline

peaks in Zif8 powder. Major peaks occur at about 7°, 10.5°, 12.5° and 24.5°. The d-spacing indicates the distance between inter-planar atoms in the lattice. In mixed matrix membrane, crystalline Zif8 particles are embedded in amorphous Torlon polymer. From the 13° peak in figure 7b), we observe that the crystalline nature of Zif8 is maintained in the Torlon-Zif8 mixed matrix membrane film.
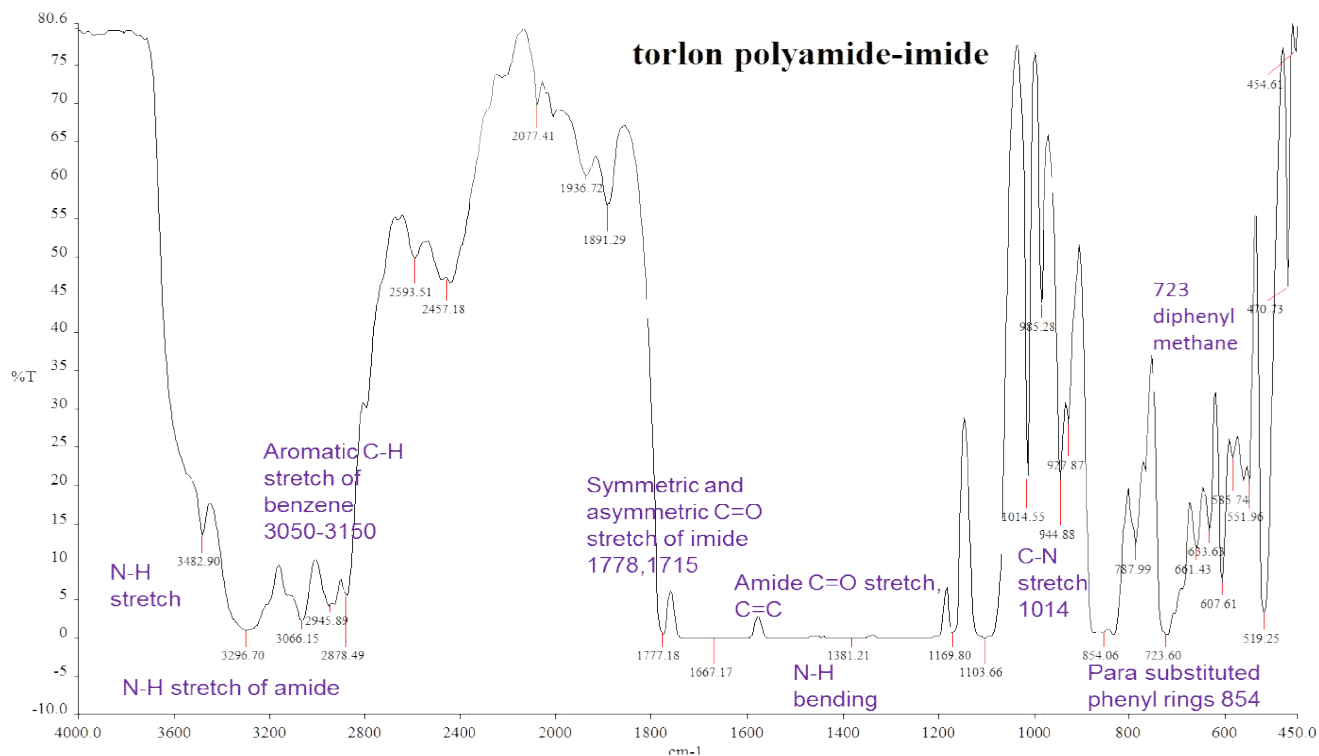

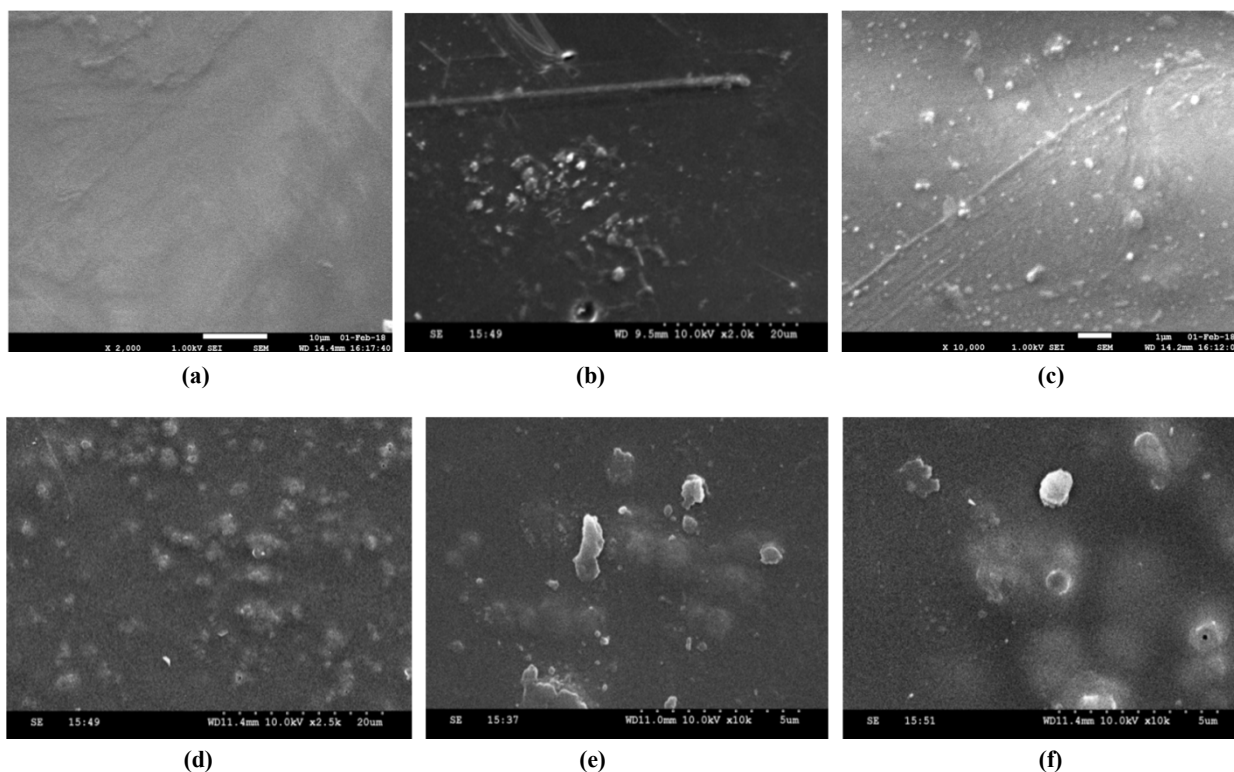**Figure 5. FTIR result on Torlon AI-10 polyamide-imide membrane**

(a)   (b)   (c)

(d)   (e)   (f)

Figure 6a,b,c,d. SEM of Torlon-ZIF8 (0%, 5%, 10%, 20%) mixed matrix membranes
Figure 6e,f. High magnification SEM of single particle-polymer interface in Torlon-ZIF8 (10%, 20%) mixed matrix membrane films

Pure gas permeation results of membranes

An isobaric gas permeation system was used to measure gas permeability, diffusion coefficient and selectivity in membrane films. Figure 8 a) is a schematic diagram of our gas permeation test system and fig.8b is a photograph of the system. Figure8b). Photograph of laboratory gas permeation measurement system built of Swagelok parts.
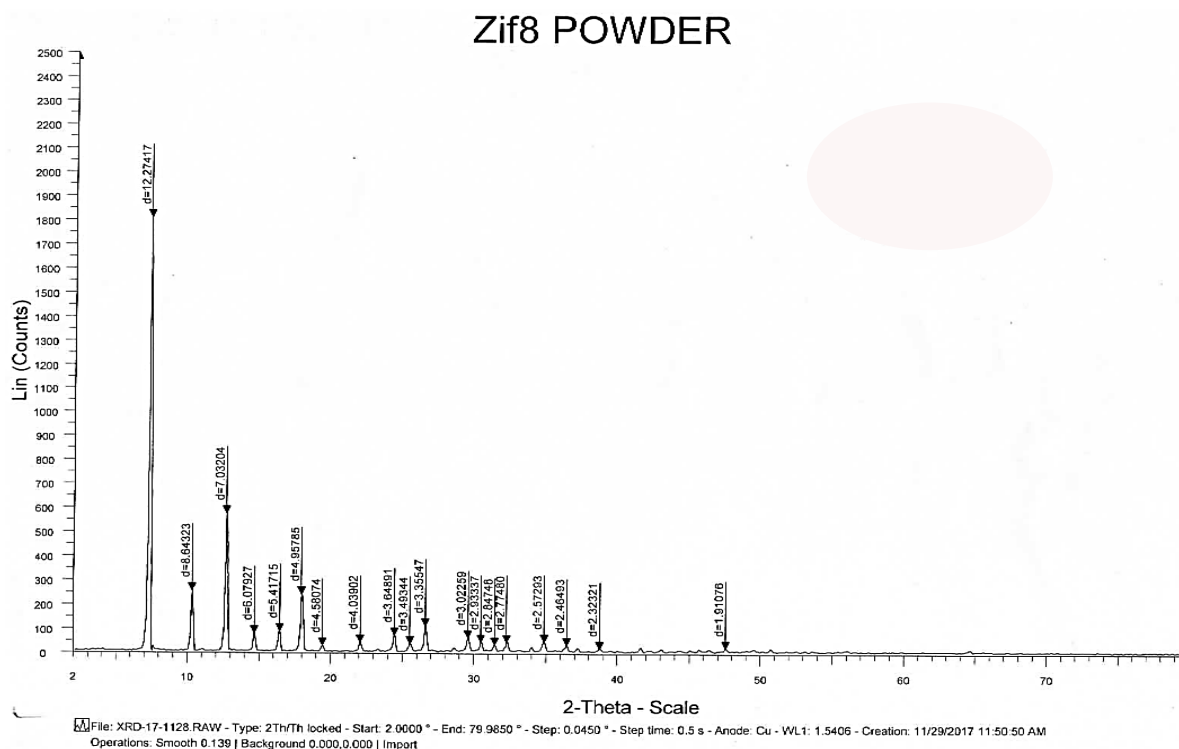
Figure 7a. X-ray diffraction analysis on pure Zif-8 powder (crystalline nanoparticles)
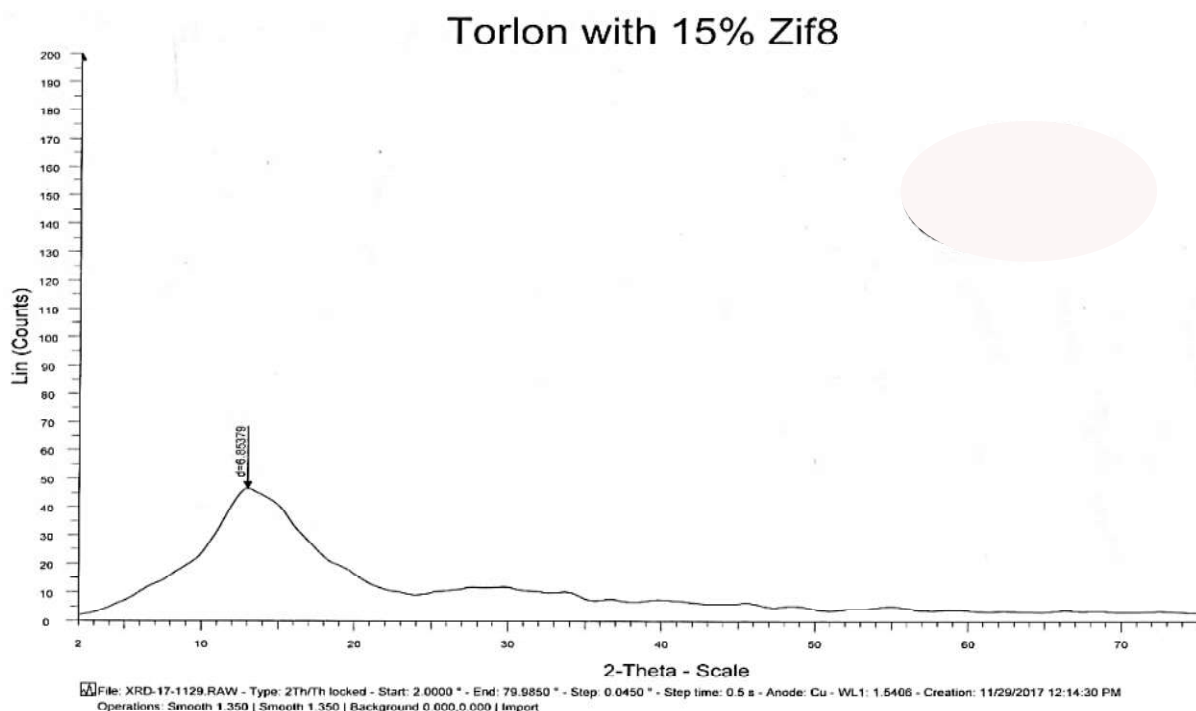

Figure 7b. X-ray diffraction analysis on Torlon-Zif8(15%) mixed matrix membrane film

Experimental procedure: A dense membrane film was tightly sealed in the gas permeation cell made of stainless steel with a sealing O-ring. The upstream retentate line is usually closed (unless retentate collection is required or retentate flow is adjusted to minimize concentration polarization). Pure gas was fed to upstream at a constant pressure between 30psia to 100psia while downstream pressure remained at ambient atmospheric 14.7psia conditions. A reshaped glass 1ml pipette (or glass 25ml burette) was connected tightly using Teflon® tape to the downstream permeate line to serve as soap bubble flow meter. When the feed valve is opened, gas permeates through the membrane. First, there is an experimental time lag noted in which the gas transport through the membrane is transitioning from unsteady state to steady state. The permeate gas starts flowing out downstream slowly. Time lag and steady state volumetric flow rate of permeate were measured using the soap bubble flow meter. Multiple (4-40) readings were taken to determine each data point. Steady state is reached within 10 time lag periods. Then, calculations were done using the following equations.
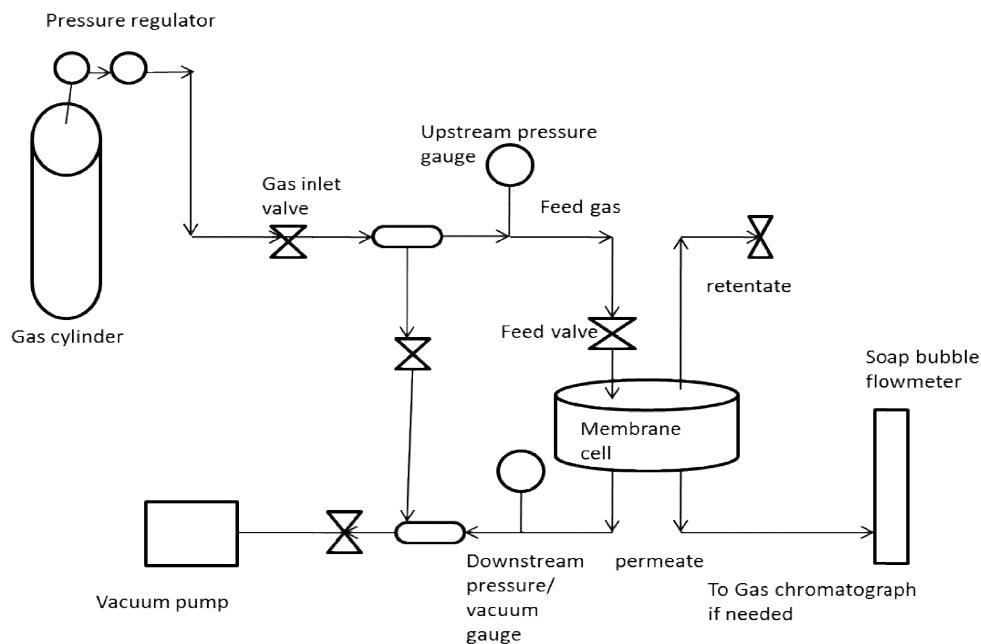
Figure 8a. Schematic diagram of isobaric gas permeation test system

Figure 8b. Photograph of laboratory gas permeation measurement system built of Swagelok parts

The permeability of the gas in the membrane at the known temperature and pressure is calculated as

$$P = \frac{(dV/dt)_{STP} \times l}{(Pup - Pdown) \times A} \qquad (6)$$

Where $(dV/dt)_{STP} = \frac{dV/dt \times 273}{(T+273)}$ is volumetric flow rate in cc/sec and downstream T is 25-30°C, l is thickness in cm, Δp is pressure difference in cm Hg (76cm Hg= 14.7 psia) and A is area in cm^2. Each experiment lasted for atleast 3 hours. Between two data points, the membrane was degassed by a vacuum pump for 2-4 hours and left in ambient air for 20 hours.

The commonly used unit of permeability is Barrer

$$1\,\text{Barrer} = 10^{-10}\,\frac{\text{cm}^3(\text{STP}) \cdot \text{cm}}{\text{cm}^2 \cdot \text{sec} \cdot \text{cm Hg}} = 3.348 \times 10^{-16}\,\frac{mol.m}{m^2.s.Pa} \qquad (2)$$

The time taken for the first soap bubble to start rise in the column was noted as time lag θ in seconds. The diffusion coefficient is calculated as D= l^2/ 6θ in cm^2/sec   (7)

Selectivity (extent of separation) is ratio of pure gas permeability values, at the same temperature as pressure.

$\alpha = Pi / Pj$ (3 a)

where Pi is permeability of gas i and Pj is permeability of gas j.

In mixed gas experiment, mixed gas feed is set at high upstream pressure and gas permeates through the membrane to the downstream. The permeate line is connected to a gas chromatograph and areas of peaks corresponding to the composition of gas present in the permeate are obtained. Separation factor of membrane is calculated as

$$\beta = \frac{y1/y2}{x1/x2}$$ (3b)

Where y1= mole fraction of gas 1 in permeate, y2= mole fraction of gas 2 in permeate, x1= mole fraction of gas 1 in feed gas and x2= mole fraction of gas 2 in feed gas.

RESULTS

Pure gas permeation data on Torlon membrane: Pure gas permeation data was obtained on a Torlon® dense membrane film at 25°C. Thickness of Torlon film was 0.009cm. Area of membrane was 38.465cm^2. Excellent gas separation ability was observed in the Torlon membrane film. Smaller gas molecule He (2.6Å size) permeates faster than CO_2(3.3Å) and the larger N_2(3.64Å) has very low permeation. At 60psia feed pressure, helium permeability is 4.9 Barrer, carbon dioxide permeability is 2 Barrer and nitrogen permeability is 0.05Barrer. Permeability decreases with increase in pressure due to saturation in the sorption capacity of the membrane for the penetrant. As pressure increases, dual mode adsorption leads to decrease in permeability (equation 8). High selectivity for CO_2/N_2 of 30-40 was obtained. Very high selectivity of He/N_2 of 56-122 was obtained. Presence of imide, aromatic groups, rigid polymer chains and interchain hydrogen bonding leading to closely packed chains that have restricted vibrations, in Torlon polyamide-imide contribute to high selectivity.

$$C = k.p + \frac{C_H.b.p}{1+b.p} \text{ and } S = C/p$$ (8)

where C=adsorption capacity, S= adsorption coefficient, p=equilibrium pressure, k= Henry's law constant, C_H= Langmuir capacity and b= Langmuir affinity constant. Total adsorption is the sum of Henry's law adsorption and Langmuir adsorption, in polymeric membranes.
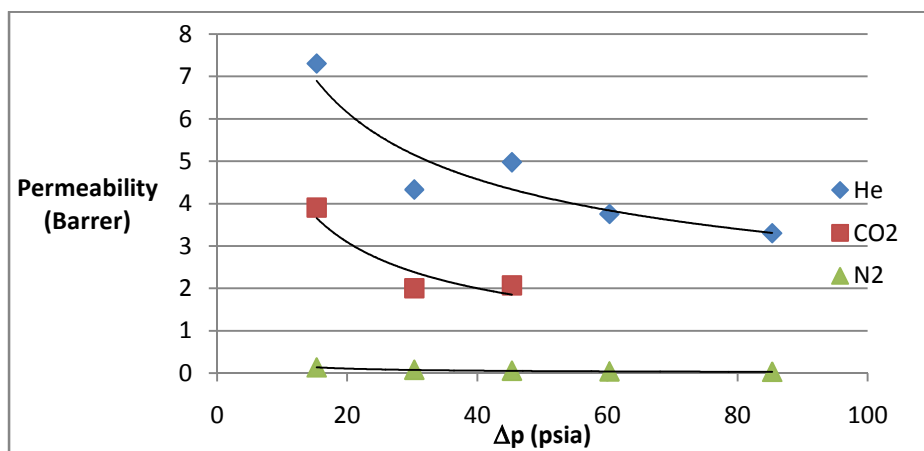

Figure 9. Pure gas permeability values in Torlon AI-10 polyamide-imide dense membrane film, as a function of pressure
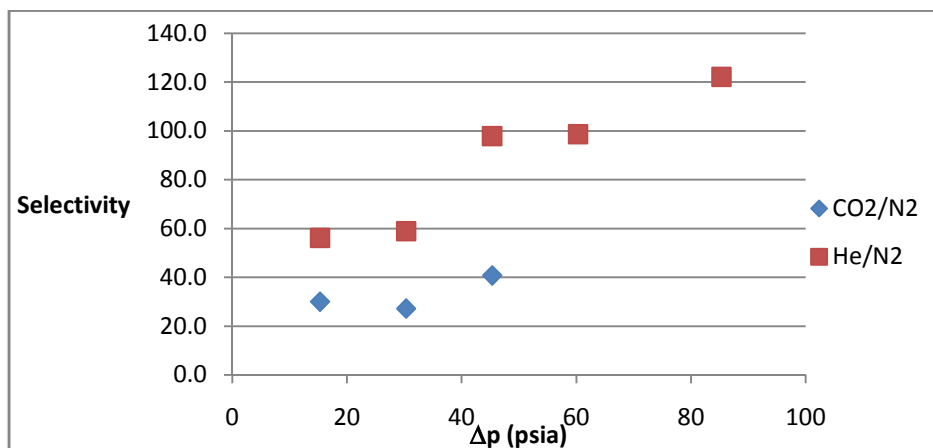

Figure 10. Carbon dioxide/nitrogen selectivity and helium/nitrogen selectivity in Torlon AI-10 membrane film, as a function of pressure

The gas pair selectivity values increase with increase in pressure. The permeability values are novel to literature. Data on Torlon® membrane film is presented in Figure 9, figure 10 and listed in table 5. Diffusivity of Helium is about 10^{-7} cm^2/sec, carbon dioxide is 10^{-8} cm^2/sec and nitrogen is 10^{-9} cm^2/sec. A selectivity of 97 implies a 98.9% pure He permeate stream if feed were a helium-nitrogen mixture.

Table 5. Pure gas permeation data on Torlon polyamide-imide membrane film

Gas	Pup (psia)	Δp (psia)	Permeability (Barrer)		Diffusivity (cm^2/sec)	Adsorption coefficient S (cc(STP)/cc.cmHg)
Helium	30	15.3	7.306	±0.25	1.022×10^{-7}	7.15×10^{-3}
Helium	45	30.3	4.33	±0.73	7.14×10^{-8}	6.06×10^{-3}
Helium	60	45.3	4.975	±0.58	9.24×10^{-8}	5.38×10^{-3}
Helium	75	60.3	3.752	±0.32	1.849×10^{-7}	2.03×10^{-3}
Helium	100	85.3	3.3	±0.44	1.50×10^{-7}	2.20×10^{-3}
Gas	Pup (psia)	Δp (psia)	Permeability (Barrer)		Diffusivity (cm2/sec)	S (cc(STP)/cc.cmHg)
Carbon Dioxide	30	15.3	3.902	±0.16	2.07×10^{-8}	1.89×10^{-2}
Carbon Dioxide	45	30.3	2	±0.12	1.73×10^{-8}	1.16×10^{-2}
Carbon Dioxide	60	45.3	2.069	±0.11	2.368×10^{-8}	8.74×10^{-3}
Gas	Pup (psia)	Δp (psia)	Permeability (Barrer)		Diffusivity (cm2/sec)	S (cc(STP)/cc.cmHg)
Nitrogen	30	15.3	0.13		1.61×10^{-8}	8.09×10^{-4}
Nitrogen	45	30.3	0.0735		8.823×10^{-9}	8.33×10^{-4}
Nitrogen	60	45.3	0.0508		2.045×10^{-8}	2.48×10^{-4}
Nitrogen	75	60.3	0.038		1.1268×10^{-8}	3.37×10^{-4}
Nitrogen	100	85.3	0.027		8.43×10^{-9}	3.20×10^{-4}

Δp (psia)	Selectivity CO_2/N_2	He/N_2
15.3	30.0	56.2
30.3	27.2	58.9
45.3	40.7	97.9
60.3		98.7
85.3		122.2

Pure gas permeation data on polyethersulfone membrane: Pure gas permeation data was obtained on a polyethersulfone (PES) dense membrane film at 25°C in 30-100psia. Thickness of membrane=0.011cm and area of membrane=38.465cm^2. Moderate gas separation ability was observed in polyethersulfone membrane. Smaller gas molecule He (2.6Å size) permeates faster than CO_2(3.3Å) and the larger N_2(3.64Å) has low permeation. At 60psia feed pressure, He permeability is 5.14 Barrer, CO_2 permeability is 3.13 Barrer and N_2 permeability is 0.194 Barrer. High selectivity for CO_2/N_2 of 45 was obtained at 30psia and it decreased to 16 at 60psia. He/N_2 selectivity decreased from 108 at 30psia to 22 at 100psia. As pressure increases, dual mode adsorption leads to decrease in permeability. The permeability decreases with increase in pressure due to saturation in the sorption capacity of the membrane for the penetrant. Presence of aromatic groups in PES contributes to high selectivity at low pressures. But, the polymer chains in PES are relatively flexible and this leads to decrease in selectivity at high pressure. As pressure increases, the vibrations of polymeric chains increase, chain packing gets disrupted and it becomes easier for nitrogen to permeate through the membrane by solution-diffusion mechanism. This results in decrease in selectivity as pressure increases, in most polymeric membranes. But if the polymer chains are very rigid and have restricted vibrations due to tight chain packing, like in Torlon polyamide-imide, then selectivity will not decrease with increase in pressure.

Pure gas permeation data on polysulfone membrane film: Pure gas permeation data was obtained on a dense membrane film of polysulfone at 25°C in 30-100psia. Thickness of membrane=0.008cm and area of membrane=38.465cm^2. Moderate gas separation ability was observed in the polysulfone membrane film. At 60psia feed pressure, helium permeability is 8.6 Barrer, carbon dioxide permeability is 7.15 Barrer and nitrogen permeability is 0.75Barrer. CO_2/N_2 selectivity decreases from 27.6 to 9 as upstream pressure increases from 30 to 60 psia. He/N_2 selectivity decreases from 66 to 2.5 as upstream pressure increases from 30 to 100 psia. The gas pair selectivity values are low and decrease with increase in pressure. The reasons for poor gas separation of polysulfone are high fractional free volume in membrane, high flexibility of polymer chains and large intersegmental distance in chain packing.

Description of Zif8 nanoparticles: Zif-8 is zeolitic imidazolate framework-8 microporous nanoparticles. ZIF-8 crystallizes in the sodalite topology (SOD) *I*-43m cubic and consists of Zn(II) tetrahedrally coordinated to four 2-methylimidazolate linkers. Each imidazole ring has two nitrogen atoms that are bonded to zinc atoms and thus, a 3-dimensional microporous network is formed (Fig.11 a). There are 6 Zn atoms containing rings that form 'cages' and 4 Zn atoms containing rings that form connecting 'windows' (figure 11 b). Commercially available Zif-8 has a structural aperture of 3.4Å size that allows CO_2 to pass through but cannot allow N_2 to pass through, making it a suitable candidate for CO_2/N_2 separations. In figure 11, the structure represents an aperture of 3.4Å size in Zif8 that is permeable only to small gases. Secondly, the organic groups in Zif-8 particles help increase compatibility with organic polymers and interfacial defects (like sieve in a cage voids when pure zeolites are used) are eliminated. Defect free well adhered polymer-Zif8 interface is obtained. In Torlon-Zif8 mixed matrix membranes, there are strong forces of physical attraction between particles and polymer like Vanderwaal's forces, π-π cloud stacking and tendency for hydrogen bonding but there is no chemical reaction between Zif-8 and Torlon. Zif8 is hydrophobic material. Gas transport in Zif-8 follows 'molecular sieving mechanism' in which gas molecules larger than the pore aperture size are excluded. The diameter of largest sphere that can fit into a Zif8 cage is about 12Å that provides large surface area but access to this cage is restricted by the 3.4Å aperture 6 Zn containing–rings. The size of the four Zn membered rings is negligible. The rate limiting step for diffusion of guest molecules is passage through the 3.4Å aperture.
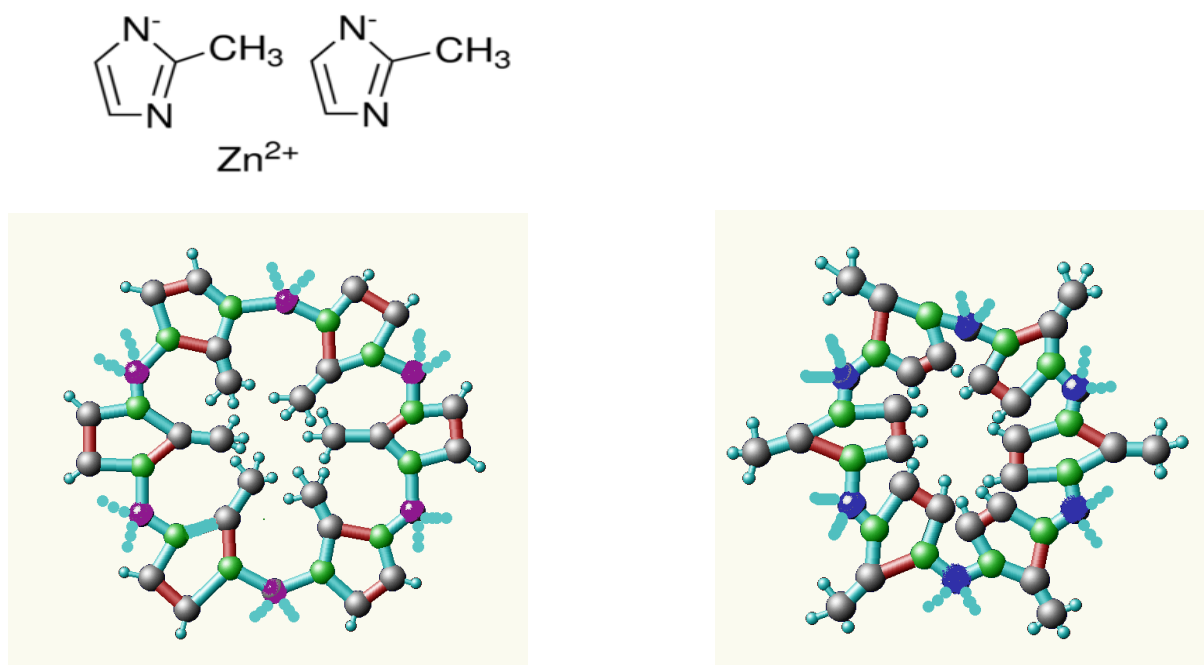
Figure 11a Molecular structure of ZIF8 aperture (3.4Å), drawn in COSMOS 6.0 (green segment is single bond and red segment is double bond)
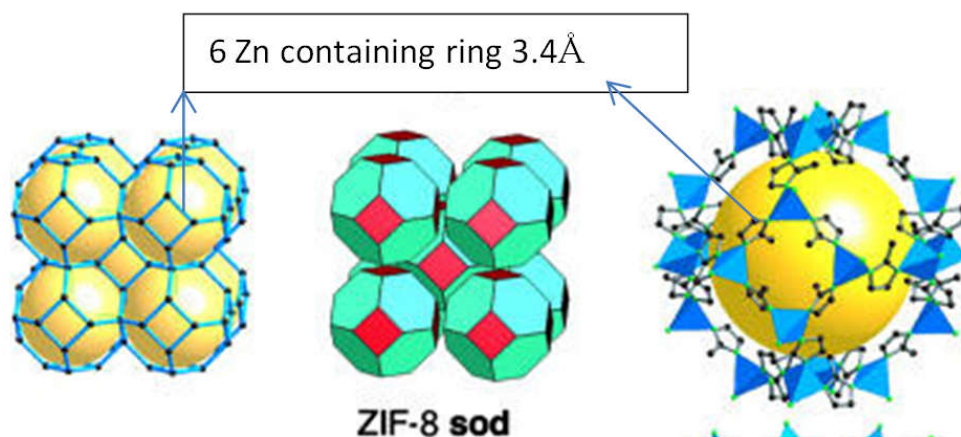

Figure 11b. Single crystal X-ray structure of Zif8 nanoparticle (re-printed with permission from PNAS (Park *et al.,* 2006), Copyright (2006) National Academy of Sciences, U.S.A)

Pure gas permeation in mixed matrix membrane Torlon-Zif8(5%): Smaller gas molecule He (2.6Å size) permeates faster than CO_2(3.3Å) and the larger N_2(3.64Å) has lower permeation. At 60psia feed pressure, helium permeability is 5.45 Barrer, carbon dioxide permeability is 1.736 Barrer and nitrogen permeability is 0.06 Barrer. The permeability decreases with increase in pressure due to saturation in the adsorption capacity of the membrane for the penetrant. CO_2/N_2 selectivity decreases from 40 to 28 as upstream pressure increases from 30 to 60 psia. He/N_2 selectivity decreases from 92 to 60 as upstream pressure increases from 30 to 100 psia.

Pure gas permeation in mixed matrix membrane Torlon-Zif8 (10%): Pure gas permeation data was measured in Torlon-ZIF8 (10%) mixed matrix dense membrane film at 25°C. Thickness of membrane=0.007cm and area of membrane = $38.465cm^2$. Data is presented in figure 12 and Table 6. In Torlon-Zif8(10%) membrane, helium permeability decreases from 30-60psia due to dual mode adsorption and increases in 75-100psia to 4.8Barrer at 100psia. This indicates that the decrease in permeability by solution-diffusion mechanism is surpassed by easy permeation of He through the open pores of the Zif-8 at 75-100psia.

Table 6. Pure gas permeation data in Torlon-Zif8 (10%) mixed matrix membrane dense film

Gas	Pup (psia)	Δp (psia)	Permeability (Barrer)		Diffusivity (cm^2/sec)
Helium	30	15.3	5.9	±0.78	1.97x10^-8
Helium	45	30.3	5.16	±0.46	4.80x10^-8
Helium	60	45.3	4.06	±0.79	4.80x10^-8
Helium	75	60.3	5.34	±0.8	3.92x10^-8
Helium	100	85.3	4.838	±0.9	5.79x10^-8
Gas	Pup (psia)	Δp (psia)	Permeability (Barrer)		Diffusivity (cm^2/sec)
Carbon Dioxide	30	15.3	2.86		2.66x10^-8
Carbon Dioxide	45	30.3	1.76	±0.2	3.25x10^-8
Carbon Dioxide	60	45.3	0.936	±0.05	1.69x10^-8
Gas	Pup (psia)	Δp (psia)	Permeability (Barrer)		Diffusivity (cm^2/sec)
Nitrogen	30	15.3	0.07		4.69Ex10^-9
Nitrogen	45	30.3	0.0443		5.44x10^-9
Nitrogen	60	45.3	0.047		8.5x10^-9
Nitrogen	75	60.3	0.0356		8.5x10^-9
Nitrogen	100	85.3	0.0252		1.517x10^-8

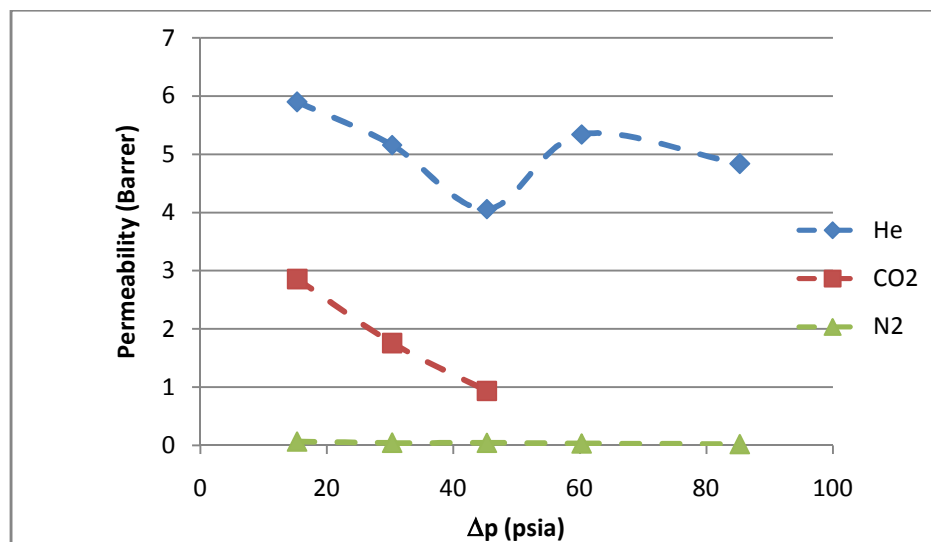| Δp (psia)	Selectivity CO_2/N_2	He/N_2
15.3	40.9	84.3
30.3	39.7	116.5
45.3	19.9	86.4
60.3		150.0
85.3		192.0

Figure 12. Pure gas permeability values in Torlon–Zif8(10%) mixed matrix membrane film, as a function of pressure

Very high He/N_2 selectivity is obtained by molecular sieving and it increases with increase in pressure: 150 at 75psia and 192 at 100psia feed pressure. Helium is able to access and permeate through most of the Zif8 particles in this membrane, in addition to through the polymer. Selectivity of 192 implies purity of 99.4% He in permeate if feed were a He-N_2 mixture. At 60 psia, CO_2 permeability is 0.93Barrer and N_2 permeability is 0.04Barrer. Carbon dioxide permeability is lower than in pure Torlon. This is because some of the pores of Zif8 are inhibited by surrounding polymeric chains (Mahajan *et al.,* 2002). Also, adsorption of CO_2 inside Zif8 is high and it does not de-sorb easily. A CO_2 molecule is very similar in size to the apertures of Zif8 and it experiences attractive and repulsive forces inside Zif8 micropore. Permeation of He and CO_2 inside Zif8 is by 'molecular sieving mechanism'; it diffuses by collisions with the walls of the micropores and transport from one cage to another via the apertures. At 30-100 psia, Zif8 acts as an impermeable filler in the polymer Torlon to N_2 and increase in the convoluted path length for permeation decreases its permeability. CO_2/N_2 selectivity is 19 at 60 psia. Open Zif8 pores are accessible only to He and CO_2 which increases the separation factor, in mixed gas feed, compared to pure Torlon. Diffusion coefficients increase with increase in pressure. Apparent adsorption coefficients decrease and become constant at medium to high pressures.

Pure gas permeation in mixed matrix membrane Torlon-Zif8(15%): In Torlon-Zif8(15%) mixed matrix membrane dense film, at 60 psia, He permeability is 4.66Barrer, CO_2 permeability is 4.21 Barrer and N_2 permeability is 0.077Barrer. Helium permeability decreases slightly from 5.6 Barrer to 4 Barrer as pressure increases from 30 to 100psia. It is a combination of solution-diffusion mechanism through the polymer and molecular sieving through Zif8. He/N_2 selectivity is 34 at 75psia and 95 at 100psia. At 45 psia, CO_2 permeability is higher than He permeability due to high adsorption of CO_2 in Zif8. This is commonly observed in microporous membranes (27, Bighane et.al. (2011)] that have high adsorption of CO_2 at room temperature as the S value in equation 1 is higher for CO_2 than He. Carbon Dioxide permeates through both the polymer Torlon and through the Zif8 micropores. Nitrogen permeability varies from 0.18Barrer at 30 psia to 0.042 Barrer at 100psia. Due to large size, N_2 cannot fit through the Zif8 particles and permeates primarily by solution-diffusion through the polymer phase. Very high CO_2/N_2 selectivity of 54.7 is observed at 60 psia.

Pure gas permeation in mixed matrix membrane Torlon-Zif8 (20%): Pure gas permeation data was measured in Torlon-ZIF8(20%) mixed matrix dense membrane film at 25°C. Thickness of membrane=0.008cm and area of membrane = 9.61cm^2. Data is presented in Figure 13.
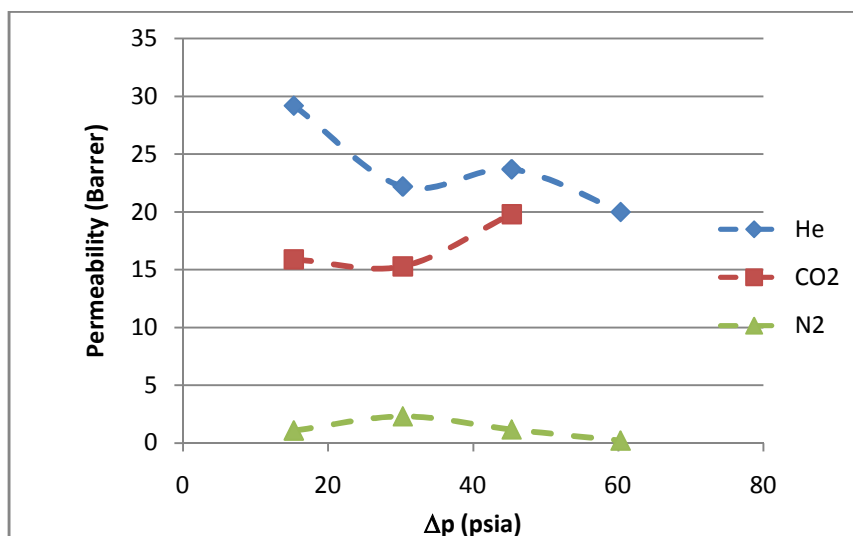

Figure 13. Pure gas permeability values in Torlon-Zif8(20%) mixed matrix membrane as a function of pressure

Torlon-Zif8 (20%) mixed matrix membrane dense film has 1) higher fractional free volume than pure Torlon and 2) has small increase in intersegmental distance in polymer chain packing due to large amount of Zif8 particles compared to pure Torlon. This imparts high helium permeability of 29.2 at 30psia and 20 Barrer at 75psia. Carbon dioxide permeability is 15.9 Barrer at 30 psia and 19.8 Barrer at 60 psia. He and CO_2 permeate through both polymer Torlon phase and through Zif8 micropores. Additionally, carbon dioxide has high adsorption in Zif8. Mechanism of permeation is a combination of solution-diffusion through the polymer and molecular sieving through Zif8. Nitrogen permeability varies from 1.07 Barrer at 30psia to 0.2 Barrer at 75 psia. N_2permeates only through the polymer phase by solution diffusion and due to increase in polymer intersegmental distance, its permeability is slightly higher than pure Torlon. Its permeability decreases due to dual mode adsorption (equation 8). N_2cannotpass through Zif8. CO_2/N_2 selectivityis 17 at 60 psia. He/N_2 selectivity is 100 at 75 psia. This membrane undergoes swelling upon application of 100 psia feed gas pressure. This membrane has exceptionally high CO_2/N_2 separation as observed in mixed gas experiments. In this manner, novel polymeric membranes were developed for flue gas separation and helium-nitrogen separation. All membrane fabrication procedures were reproducible. All gas permeation data were reproducible. All the membranes developed and studied in this paper (section 4.1-4.3, 6.2-6.8) do not exhibit aging and do not swell upon exposure to CO_2. The developed dense membrane films have a shelf life of atleast 6 months. The dense membrane films do not undergo any physical or chemical change with time.

Mixed gas separation results

The gas permeation system was assembled near a gas chromatograph. The feed line was connected to a mixed gas cylinder containing a mixture of CO_2 and N_2 (70%N_2:30%CO_2). The permeate line was connected to an online gas chromatograph Agilent 7820A GC system with a Newchrom® 16214 column inside it. GC oven temperature was 60-80°C and thermal conductivity detector was maintained at 150°C. Helium was used as carrier gas. Mixed gas permeation experiments were conducted at three feed pressures and the permeate gas was analyzed. Two peaks were obtained in the permeate streams, the first small peak corresponding to nitrogen and the second larger peak corresponding to carbon dioxide. %area gave the composition of the permeate stream. The separation factor was calculated used equation 3b). The mixed gas permeation results on membranes are summarized in Table 7. 165 analysis runs were performed to accurately and reproducibly determine each data point. At each pressure, the experiment was held for atleast 2 hours. Upon applying mixed gas to our polymeric membranes in the range 30-60 psia, 1) the highly adsorbing carbon dioxide gas sweeps nitrogen along with it into the permeate, although the pure gas permeability of N_2 is very low. Force of attraction between CO_2 and nitrogen is called coupling effect. The gas phase interactions between CO_2 and N_2 can be a combination of dispersion, weak electrostatic and quadrupole based interactions, also involving the lone pair of N_2 (Pg.37) in (Koros *et al.,* 1993; Yeom *et al.,* 2000; Hernandez Marin 2015). 2) Secondly, the adsorption sites of CO_2 in the membrane get occupied by N_2. This is called competitive adsorption effect. Thus, permeate gets filled with about 17% nitrogen (83%CO_2) in Torlon-Zif8(5%) membrane. Mixed gas separation factor of the membrane is 11.3 for pure Torlon, 12 for Torlon-ZIF8(5%), 13.2 for Torlon-Zif8(10%) and 8.9 for polyethersulfone. Mixed gas selectivity is lower than pure gas selectivity (40 for pure Torlon) because of the above mentioned reasons. The separation factor values are novel to literature and acceptable. The separation factor of Torlon-Zif8 mixed matrix membranes is higher than that of pure Torlon. In Torlon-Zif8 membranes, although CO_2 sweeps N_2 along with it through the polymer phase, the nitrogen cannot fit to diffuse through the Zif8 particles phase while CO_2 can diffuse through both phases. Therefore, size based exclusion of N_2 in Zif8 results in high gas separation factor β values in the mixed matrix membranes. Addition of more Zif8 creates more blockages for N_2 in the membranes. In Torlon-Zif8(20%) mixed matrix membrane film, 99.8% pure CO_2 permeate stream was obtained. This excellent result justifies the addition of Zif8 to Torlon to obtain a highly selective gas separation membrane. In addition to size-based exclusion of N_2, competitive adsorption of CO_2 higher than N_2 in Torlon-Zif8(20%) also contributes to high gas separation.

Table 7. Mixed gas separation data on studied membranes, as a function of pressure

Membrane	feed gas pressure (psia) 3/7=0.428	GAS	retention time (minutes) Permeate gas analysis by GC	Area of peaks	area%	CO_2/N_2 separation factor of membrane
1. Polyethersulfone	60	N_2	0.693	11858350	20.78	
		CO_2	1.173	45213171	79.22	8.9
	45	N_2	0.724	7837218	18.86	
		CO_2	1.207	33723674	81.14	10
	30	N_2	0.705	1530023	21.01	
		CO_2	1.195	5752092	78.99	8.7
2. Torlon	60	N_2	0.708	6456254	17.04	
		CO_2	1.188	31443654	82.96	11.3
	45	N_2	0.713	1544832	21.15	
		CO_2	1.203	5759056	78.85	8.7
	30	N_2	0.715	1564879	20.78	
		CO_2	1.205	5964068	79.21	8.9
3. Torlon- ZIF8 (5%)	60	N_2	0.708	6600779	16.23	
		CO_2	1.191	34057720	83.75	12
	45	N_2	0.715	4483723	17.49	
		CO_2	1.198	21147809	82.51	11
	30	N_2	0.7	4117952	15.73	
		CO_2	1.183	22057851	84.27	12.5
4. Torlon-Zif8(10%)	60	N_2	0.684	2919709	15.01	
		CO_2	1.151	16530777	84.99	13.2
5.Torlon-Zif8(15%)	60	N_2	0.691	3838534	16.62	
		CO_2	1.161	19262614	83.38	11.7
6. Pure Torlon after exposure to Steam	60	N_2	0.656	2355380	5.96	
		CO_2	1.116	37147315	94.04	36.8
	45	N_2	0.501	2529465	9.52	
		CO_2	0.964	24034653	90.48	22.2
	30	N_2	0.685	2862681	12.56	
		CO_2	1.152	19922960	87.44	16.2
7. Torlon-Zif8(20%)	60	N_2	0.690	38306	0.12	
		CO_2	1.166	32338657	99.88	231
	45	N_2	0.689	34319	0.11	
		CO_2	1.153	31399722	99.89	231
	30	N_2	0.691	42815	0.14	
		CO_2	1.144	31032101	99.86	231

Membrane Technology and Research, Inc. successfully demonstrated their Polaris® membrane retrofitted to a 1MW coal fired plant and obtained 65% CO_2 in permeate from primary step (43, Merkel et.al.(2017). They plan to compress the permeate to supercritical CO_2 liquid. After second stage membrane, they vented retentate of 2% CO_2. Pilot plant studies on a fixed site carrier (facilitated transport) membrane of polyvinylamine (45, Sandru et.al.(2013)] gave 75% CO_2 in permeate stream. Higher CO_2/N_2 mixed gas selectivity of 19 for 6FDA-DAM/DABA polyimide membrane (Lively *et al.,* 2012), 10 for membranes in NCCC (Kusuma *et al.,* 2017) and about 20 for membranes in NETL have been reported (47Venna et.al. (2017). Ultem with Zif8 membranes (Dai *et al.,* 2012) provide CO_2/N_2 mixed gas selectivity of 20-30. 1,6- hexane diamine-crosslinked polyurethane has mixed gas CO_2/N_2 selectivity of 17 (Ishafahani *et al.,* 2016). Gas separation performance of Torlon membranes was unaffected by exposure to steam.

Mechanism of gas transport in polymeric membranes: Gas transport through polymeric membranes is governed by the 'solution-diffusion mechanism', dependent on chain mobility and involving molecular adsorption of the gas between polymeric segments. P=DxS

Permeability P= DxS

where D=diffusion coefficient and S=adsorption coefficient.

Energy of molecule U

Energy required for expanding chain to make a transient gap, Ed

Energy required to overcome sorption and make a jump, ΔHs
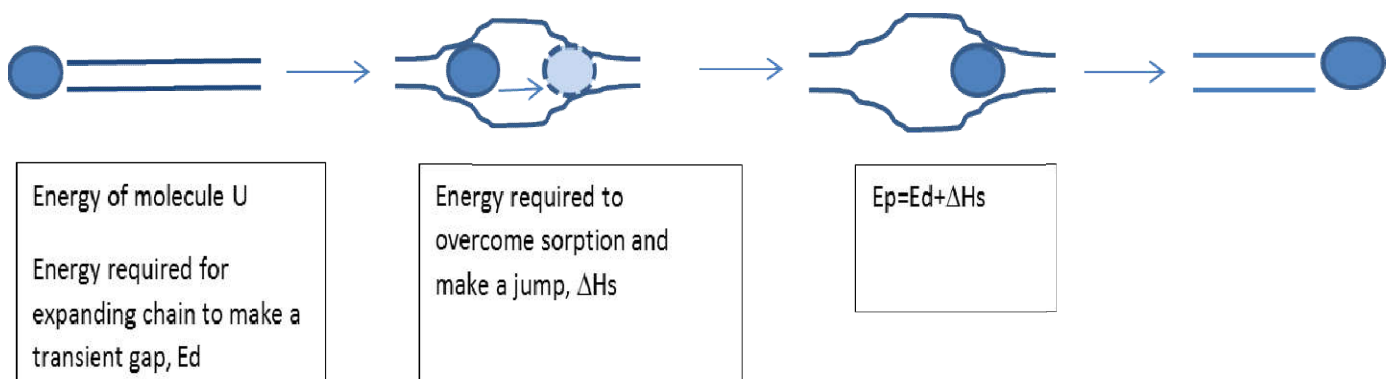
$Ep=Ed+\Delta Hs$

Figure 14. Diagram of permeation of a gas molecule in a polymer by solution-diffusion model

_____

E_d represents the activation energy of diffusion of a gas for a molecule to cause opening of a temporary gap between two entangled polymeric chains. ΔHs is the enthalpy of adsorption of a gas as it jumps from one adsorption site to another in a polymer. Ep is the activation energy of permeation. The thermally agitated motion of chain segments comprising the polymer matrix generate penetrant-scale transient gaps by which pressure-driven adsorbed gas molecules diffuse from the upstream to the downstream face of the membrane (Koros *et al.,* 1988; Koros *et al.,* 1993). Diffusion coefficient represents how often and how far a gas molecule can jump in the membrane, at the given pressure difference and temperature.

$$D= f\lambda^2/6 \qquad\qquad\qquad (9)$$

where f= frequency of jump and λ= jump length (Hines *et al.,* 1985).

Permeability represents the number of gas molecules passing through a unit area of the membrane per unit time, at the set pressure difference across the thickness of the membrane at STP (standard temperature and pressure: 273K and 1atm) and set temperature. In microporous particles of Zif8, the mechanism of gas permeation is 'molecular sieving'. The framework of the pores is rigid and the gas molecules adsorb, collide with pore walls to diffuse forward and de-sorb for permeation. In molecular sieving, the size of the pores are similar to the size of the gas molecules and gas molecules larger than the pores are not able to diffuse through the particles. In Torlon-Zif8 mixed matrix membranes, gas permeation is a combination of solution-diffusion and molecular sieving. Small gas molecules such as He and CO_2 permeate faster through the Zif8 pores than through entangled chains of polymer Torlon. It is depicted in Figure 16.
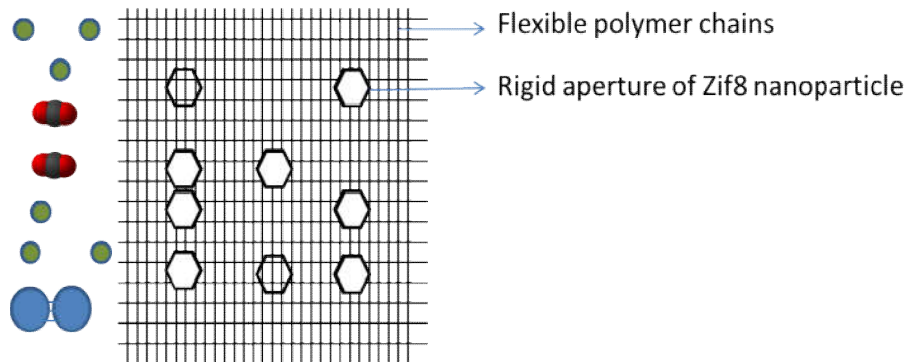

Figure 15. Diagram of micromorphology of Torlon-Zif8 mixed matrix membrane films
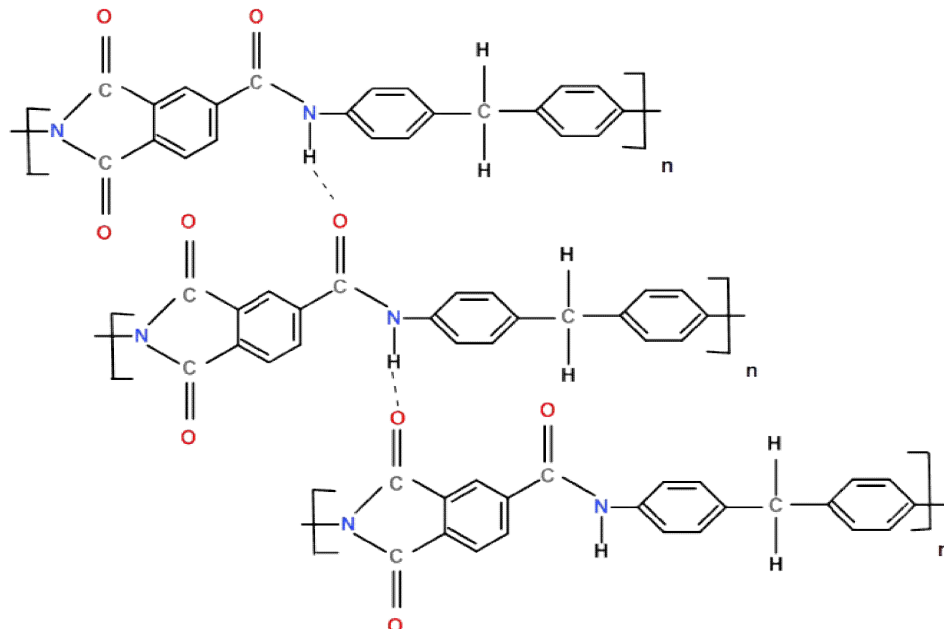

Figure 16. Diagram of inter-chain hydrogen bonding in Torlon AI-10 polymer membrane

In 10% Zif8 in Torlon membranes, nitrogen cannot permeate through Zif8 particles due to size based exclusion. Molecular sieving through Zif8 provides high He/N_2 selectivity=192 and moderate CO_2/N_2 separation factor. In 20% Zif8 in Torlon membranes, open pores of most Zif8 particles are accessible to helium and carbon dioxide. This results in increase in permeability of He and CO_2 compared to pure Torlon. Nitrogen cannot permeate through Zif8 particles due to size based exclusion. Molecular sieving through Zif8 provides high selectivity for CO_2/N_2 separation. The main advantage of more Zif8 is evident in highest purity 99.8%CO_2 in permeate obtained from Torlon-Zif8(20%) membrane from CO_2-N_2 mixed gas feed.

Uses of captured gas streams

As intended, feed flue gas stream would contact a membrane unit and separate into CO_2 permeate stream and N_2 retentate stream. The separated gas streams can be used for various purposes. CO_2 is can be used in the production of urea, production of methanol, carbonates and bicarbonates, like washing soda and baking soda. It is also used in fire extinguishers, supercritical solvent and as solid refrigerant. Plants absorb CO_2 for photosynthesis. Nitrogen is used in the Haber's process for production of ammonia for fertilizers. It is also used in propellants, explosives, organic compounds like Kevlar fabric and pharmaceutical drugs. Nitrogen occurs in organisms in amino acids, proteins, nucleic acids and in the energy transfer molecule adenosine triphosphate. The nitrogen cycle involves movement of nitrogen from air to the biosphere and organic compounds and back to the atmosphere. From the experimentally observed purity of permeate stream($83\%CO_2$-$17\%N_2$) in single stage membrane mixed gas experiments, our Torlon and Torlon-Zif8(5% or 10% or 15%) membranes can provide CO_2 for applications such as: modified atmosphere packaging, chilling, freezing and temperature control of foods and beverages, pH control in industrial site process water and waste water treatment, shielding gas in semi-automatic welding process, arc-welding, plasma cutting, metal heat treatment in automotive industry, metal cryogenic treatment, calibration gas mixture for engine emissions testing in automotive industry and in upstream oil and gas industry for Enhanced Oil Recovery (injected supercritical CO_2 dissolves and decreases viscosity of oil in wells enabling easy extraction) and hydraulic fracturing (CO_2-N_2 mixture is sent at high pressure to create fissures in underground wells to release entrapped oil or gas) (Air Liquide, 2018). With 99.8% purity, Torlon-Zif8 (20%) membranes can provide CO_2 for applications such as: Draft gas passed through beer in breweries to enhance taste, quality (CO_2) and shelf life (N_2), carbonation in soft drinks to provide effervescence and enhance shelf life, modified atmosphere packaging of foods and beverages, fire extinguishers, automotive industry and in upstream oil and gas industry for enhanced oil recovery (Air Liquide, 2018). Use of CO_2 gas in food and beverage industry requires Food Safety System Certification 22000 (FSSC 22000). There is also interest in carbon capture and storage (sequestration). Captured CO_2 can be stored underground like in the Sleipner West field in North sea or Weyburn field.

DISCUSSION

In common polymer membranes like polyethersulfone and polysulfone, gas selectivity for CO_2/N_2 and He/N_2 decrease with increase in pressure. This is due to flexibility of polymeric chains and disruption in chain packing at high pressures. Large molecules like N_2 are able to permeate through these membranes at high pressures and this leads to decrease in selectivity. However, this trend can be reversed if 1) the chains are molecularly stiff (like with aromatic groups) and 2) the chains are rigidly packed by inter-chain cross-links or inter-chain hydrogen bonding. Torlon AI-10 has a molecularly rigid chain structure. In addition, as observed in polymer Torlon, which also has inter-chain hydrogen bonding, the selectivity values increase with increase in pressure because the polymeric 'chain packing' remains rigid/intact even at high pressures. This is depicted in Figure 16. Research efforts for flue gas capture are challenging due to low CO_2 partial pressure driving force in mixed gas at 50°C, sometimes saturated with water. The enormous volume of a power plant flue gas stream means very large membrane areas are required for processing the gas. While gas transport property is important, it is also necessary that the membrane material be strong, durable, resistant to chemical corrosion and resistant to plasticization.. Ryan Lively *et al.* estimated that a membrane area of 3.4million m^2 of polyimide 6FDA-DAM:DABA(4:1) hollow fibers compacted as 13070 modules (8" diameter, $8000m^2/m^3$) are needed to capture CO_2 in one 600MW coal power plant (Lively *et al.,* 2012). Single stage and multi- step, multi-stage designs incorporating counter-flow sweep membrane module model operation calculations, with effect of feed compression or vacuum on permeate on membrane area and cost, were illustrated for flue gas capture by Merkel *et al.* The required optimum membrane CO_2/N_2 selectivity falls in the range 20-40 (Merkel *et al.,* 2010). Carbon capture consumes energy from the host plant. The U.S. Department of Energy (DOE) has set the target of less than 35% increase in the cost of electricity (COE) for 90% CO_2 capture from power plants. A well-known technique of CO_2 capture is by absorption/stripping in amine based solvents. It is most efficient at the Petra Nova carbon capture facility (eia.gov 2018) (about 80MW consumed for 240MW generated). It is estimated that, for one power plant, the cost for pure polymeric membrane units will be 8-27% of the investment for absorption in amine solutions. Pure Torlon AI-10 film membrane costs $91/m^2$. Cost for Torlon-Zif8(20%) film membranes is $2125/m^2$ with estimated required area 0.262million m^2 for one power plant, 19Barrer CO_2 permeability, 70µm thickness, 10min residence time of feed gas as in fig.1 for feed gas of $500m^3$ containing 20% CO_2 at Δp=60-14.7= 45.3psia. The cost of asymmetric Torlon-Zif8(20%) membranes with 1µm separating layer will be $7.9million excluding the support layer which can be made of pure Torlon. This can be achieved by dual layer hollow fiber spinning (or thin film coating on compatible inexpensive support). Helium is used in MRI scanners, semi-conductors, fiber optic cables, space exploration, scientific research, air-bag production, professional hyperbaric diving, leak detection and balloons. In Torlon based membranes studied in this paper, exceptionally high selectivity for helium/nitrogen has been observed that can enable helium separation processes and significantly reduce cost. The developed Torlon-Zif8 membranes also provided high CO_2/CH_4 separation. The performance of the studied membranes is plotted on the Robeson upper bound curve in figures 17 and 18 (Robeson, 2008) (background re-printed with permission from Elsevier, license no. 4234710132221). Red circles are data points of various membranes in literature. The black line represents the trade-off curve for CO_2/N_2 separation and for He/N_2 separation. The key parameters for gas separation by a membrane are its permeability of faster component in a mixture and the selectivity. It has been recognized that these two are trade-off parameters as the selectivity generally decreases with increasing permeability of the more permeable gas component.

$$P_i = k.\alpha_{ij}^n \qquad\qquad (10)$$

For CO_2/N_2 separation, k=30,967,000 Barrer and n=-2.888.

For He/N_2 separation, k=19,890 Barrer and n= -1.017.
Performances of developed membranes lie in the high selectivity region of the upper bound plot.
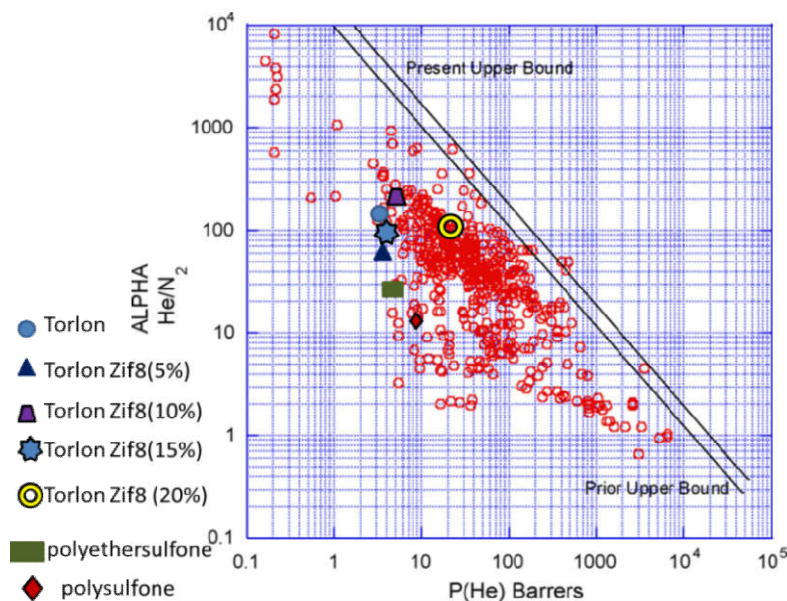

Figure 17. Gas separation performance of studied membranes on the Robeson upper bound curve for helium-nitrogen separation (background re-printed with permission from Elsevier)
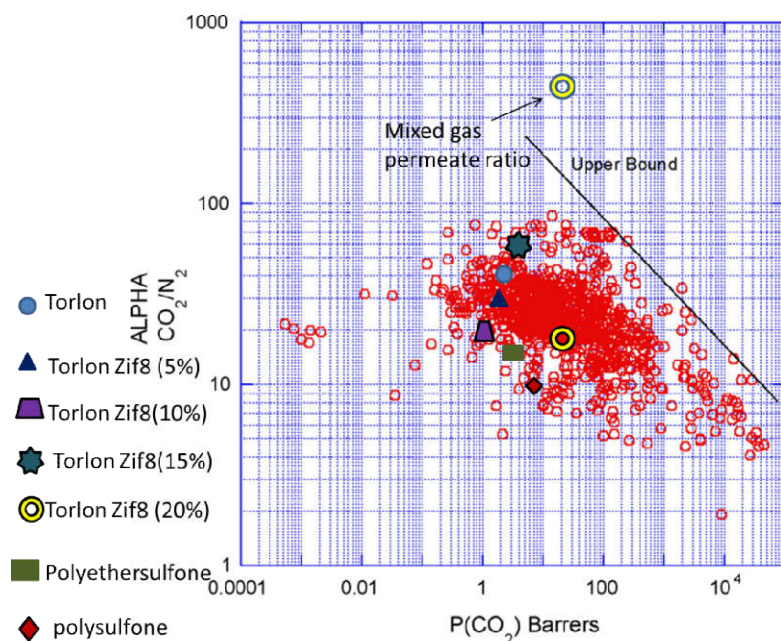

Figure 18. Gas separation performance of studied membranes on the Robeson upper bound curve for carbon dioxide-nitrogen separation (background re-printed with permission from Elsevier)

Summary and conclusion

Polymeric membranes of three different glassy polymers and novel mixed matrix membranes were studied for application to carbon dioxide-nitrogen separation and helium-nitrogen separation. Dense membrane films (about 300cm^2 area) of polymers were fabricated by solution casting and complete evaporation of solvent technique. The thickness of the membrane films was 0.07-0.11mm. Puregas permeation data and mixed gas separation data was experimentally compiled. Torlon® AI-10 membrane has pure gas CO_2/N_2 selectivity of 40 and He/N_2 selectivity of 97 at 60 psia. The developed membranes are strong, flexible, durable, can withstand 75psia gas pressure and provide good gas separation. Best performance for helium-nitrogen separation was observed in Torlon-Zif8(10%) mixed matrix membranes with selectivity 192 at 100psia. Best performance for CO_2/N_2separation was observed in Torlon-Zif8(20%) mixed matrix membranes with 99.8% pure CO_2 permeate stream at 60psia, from mixed gas feed. The developed Torlon membranes are robust polymeric materials that can enable flue gas separation and helium- nitrogen separation to high purity. As global warming is increasing, there is an urgent need to focus attention towards reducing CO_2 emissions into the atmosphere and membranes can play a vital role in this situation. Although amine absorption and cryogenic distillation are mature technologies, they require large amounts of energy for operation. Membranes operate by pressure difference and can lower cost to improve efficiency in industrial processes like flue gas capture or helium separation.

REFERENCES

Ali Pournaghshb and Isfahani, Behnam Ghalei, Kazuki Wakimoto, Rouhollah Bagheri, Easan Sivaniah and Morteza Sadeghi, Plasticization resistant crosslinked polyurethane gas separation membranes, J. Mater. Chem. A,4 (2016) 17431

Andrew J. Brown, Nicholas A. Brunelli, Kiwon Eum, Fereshteh Rashidi, J. R. Johnson, William J. Koros, Christopher W. Jones, Sankar Nair, 2014. Interfacial microfluidic processing of metal-organic framework hollow fiber membranes, *Science,* Vol. 345, Issue 6192, 04, 72-75

Anthony L. Hines, Robbert N. Maddox, Mass Transfer-fundamentals and applications, Prentice-Hall, Inc., 1985.

Carter D., H.F. Tezel, B. Kruczeck, H. Kalipcilar, 2017. Investigation and comparison of mixed matrix membranes composed of polyimide matrimid with ZIF – 8, silicalite, and SAPO – 34, *Journal of Membrane Science,* 544, 35–46.

Clem E. Powell, Greg G. Qiao, Polymeric CO_2/N_2 gas separation membranes for the capture of carbon dioxide from power plant flue gases, *Journal of Membrane Science,* Volume 279, Issues 1–2, 1 August 2006, Pages 1–49.

Colin A. Scholes, Joannelle Bacus, George Q. Chen, Wen X. Tao, Gang Li, Abdul Qader, Geoff W. Stevens, Sandra E. Kentish, 2012. Pilot plant performance of rubbery polymeric membranes for carbon dioxide separation from syngas, *Journal of Membrane Science*, 389, 470– 477.

Colin A. Scholes, Ujjal Ghosh, 2016. Helium separation through polymeric membranes: selectivity targets, Journal of Membrane Science 520, 221–230.

David S. Sholl, Ryan P. Lively, 2016. Seven chemical eparations to change the world, *Nature,* 532 (2016), 435-437.

De Vos, R.M., Henk Verweij, 1998. Improved performance of silica membranes for gas separation, Journal of Membrane Science, 143, 37-51.

Elizabeth Hernández-Marín, Ana Adela Lemus-Santana, 2015. Theoretical Study of the Formation of Complexes Between CO_2 and Nitrogen Heterocycles, *J. Mex. Chem. Soc.,* 59(1), 36-42.

Eric Favre, Carbon dioxide recovery from post-combustion processes: Can gas permeation membranes compete with absorption?, *Journal of Membrane Science,* 294 (2007) 50–59.

Gary T. Rochelle, 2009. Amine scrubbing for CO_2 capture, Science, Vol.325, Issue 5948, 1652- 1654.

Houghton, J.T. Climate Change 2001: The Scientific Basis, Cambridge University Press, Cambridge, 2001

John D. Perry, Kazukiyo Nagai, and William J. Koros, 2016. Polymer membranes for hydrogen separations, MRS Bulletin, Volume 31.

Junyi Liu, Xianda Hou, Dr. Ho Bum Park, Dr. Haiqing Lin, 2016. High-Performance Polymers for Membrane CO_2/N_2 Separation, Chemistry: *A European Journal,* Volume 22/45, 15980–15990

Kanezashi M., Masashi Asaeda, 2006. Hydrogen permeation characteristics and stability of Ni-doped silica membranes in steam at high temperature, Journal of Membrane Science 271, 86-93.

Kevin O Brien, W.J. Koros, 1988. Polyimide materials based on pyromellitic dianhydride for the separation of carbon dioxide and methane gas mixtures, Journal of membrane science, 35, 217-230.

Koros W.J., G.K. Fleming, Membrane-based gas separations, Journal of Membrane Science, 83, l-80.

Koros W.J., Ryan P. Lively, 2012. Water and beyond- expanding the spectrum of large-scale energy efficient separation processes, AIChE journal, Vol.58, No.9, 2624-2633.

Koros, W.J., G.K. Fleming, S.M. Jordan, T.H. Kim, H.H. Hoehn, 1988. Polymeric membrane materials for solution-diffusion based permeation separations, Progress in Polymer Science, Vol. 13, 339-401.

Kyo Sung Park, Zheng Ni, Adrien P. Coˆ te´, Jae Yong Choi, Rudan Huang, Fernando J. Uribe-Romo, Hee K. Chae, Michael O'Keeffe, and Omar M. Yaghi, 2006. Exceptional chemical and thermal stability of zeolitic imidazolate frameworks, Proceedings of the National Academy of Sciences, Vol.103, no.27, 10186-10191.

Llyod M.Robeson, 2008. The upper bound revisited, Journal of Membrane Science 320, 390–400.

Louei A. El. Azzami, Eric A. Grulke, 2009. Carbon dioxide separation from hydrogen and nitrogen Facilitated transport in arginine salt-chitosan membranes, *Journal of membrane science,* 328,15-22.

Lu Liu, Wulin Qiu, Edgar S. Sanders, Canghai Ma, William J. Koros, 2016. Post-combustion carbon dioxide capture via 6FDA/BPDA-DAM hollow fiber membranes at sub-ambient temperatures, Journal of Membrane Science 510, 447–454.

Madhava R. Kosuri, 2009. Polymeric Membranes for Super Critical Carbon Dioxide (scCO₂) Separations, Ph.D. thesis, Georgia Institute of Technology.

Madhava R. Kosuri, William J. Koros, 2008. Defect-free asymmetric hollow fiber membranes from Torlon®,a polyamide–imide polymer, for high-pressure CO2 separations, *Journal of Membrane Science*, 320, 65–72.

Marius Sandru, Taek-Joong Kim, Wieslaw Capala, Martin Huijbers, May-Britt Hägg, 2013. Pilot Scale Testing of Polymeric Membranes for CO_2 Capture from Coal Fired Power Plants, *Energy Procedia,* Vol. 37, 6473-6480.

Mark Maslin, Global warming: a very short introduction, Oxford university press, 2004.

Mayumi Kiyono, 2010. Carbon molecular sieve membranes for natural gas separations, Ph.D. thesis, Georgia Institute of Technology.

McCarthy J.J., O.F. Canziani, N.A. Leary, D.J. Dokken, K.S. White, Climate Change 2001: Impacts, Adaptation, and Vulnerability, Cambridge University Press, Cambridge, 2001.

Melinda L. Jue, Victor Breedveld, Ryan P. Lively, 2017. Defect-free PIM-1 hollow fiber membranes, Journal of Membrane Science 530, 33–41.

Neha Bighane, 2012. Novel silica membranes for high temperature gas separations, M.S. thesis, Georgia Institute of Technology.

Neha Bighane, 2017. Novel silica and silica-titania membranes for high temperature gas separations, 8th Annual congress on Analytical and Bioanalytical techniques, Brussels, Belgium, 28-30.

Neha Bighane, W.J. Koros, 2011. Novel silica membranes for high temperature gas separations, Journal of membrane science, 371, 254-262.

Neha Bighane, W.J. Koros, Novel silica-titania membranes, Invention disclosure GTRC 6456, August 2013, Georgia Tech Research Corporation, Dow Corning Corporation.

O.Davidson, B., Metz *et al.,* 2005. Special Report on Carbon Dioxide Capture and Storage, International Panel on Climate Change, Geneva, Switzerland, www.ipcc.ch

Pacala S., R. Socolow, Stabilization wedges: solving the climate problem for the next 50 years with current technologies, Science 305 (2004)968.

Peinemann K.V., K.Fink, P.Witt, 1986. Asymmetric polyetherimide membrane for helium separation, Journal of Membrane Science, 27, 215-216.

Rajiv Mahajan, William J. Koros, 2002. Mixed Matrix Membrane Materials With Glassy Polymers. Part 2, *Polymer Engineering and Science,* Vol.42, No.7.

Ralph T. Yang, Adsorbents: Fundamentals and applications, 2003 John Wiley and Sons., Inc.

Raymond W. Chafin, Torlon and Silicalite mixed matrix membranes for xylene isomer purification, Ph.D. Thesis, Georgia Institute of Technology, May 2007.

Ryan P. Lively, 2011. Hollow fiber sorbents for post-combustion CO_2 capture, Ph.D. thesis, Georgia Institute of Technology.

Ryan P. Lively, Ronald R. Chance, B. T. Kelley, Harry W. Deckman, Jeffery H. Drese, Christopher W. Jones and William J. Koros, 2009. Hollow Fiber Adsorbents for CO_2 Removal from Flue Gas, Industrial and Engineering Chemistry Research 48, 7314–7324

Ryan P.Lively, Michelle E.Dose, LirenXu, JustinT.Vaughn, J.R. Johnson, Joshua A.Thompson, Ke Zhang, Megan E. Lydon, Jong-Suk Lee, LuLiu, Zushou Hu, O^guz Karvan, Matthew J. Realff, William J. Koros, 2009. A high-flux polyimide hollow fiber membrane to minimize footprint and energy penalty for CO_2 recovery from flue gas, Journal of Membrane Science 423– 424, 302–313.

Solomon, S., D. Qin, M. Manning, Z. Chen, M. Marquis, K.B. Averyt, M. Tignor and H.L. Miller (eds.), IPCC, 2007. Summary for Policymakers. In: *Climate Change 2007: The Physical Science Basis. Contribution of Working Group I to the Fourth Assessment Report of the Intergovernmental Panel on Climate Change,* Cambridge University Press, Cambridge, United Kingdom and New York, NY, USA.

Surender Venna, Experiemental materials development in mixed matrix membranes for post-combustion carbon capture, 2017 DOE NETL CO_2 capture technology project review meeting.

Tim C. Merkel, H. Lin, X. Wei, Richard Baker, 2010. Power plant post-combustion carbon dioxide capture: an opportunity for membranes, *Journal of Membrane Science,* 359, 126-139.

Tim Merkel *et al.,* Integrated testing of a membrane CO_2 capture process with a coal fired boiler, 2017 DOE NETL CO_2 capture technology project review meeting.

Victor A. Kusuma, Surendar R. Venna, Shan Wickramanayake, Ganpat J. Dahe, Christina R. Myers, John O'Connor, Kevin P. Resnik, Justin H. Anthony, David Hopkinson, 2017. An automated lab-scale flue gas permeation membrane testing system at the National Carbon Capture Center, *Journal of Membrane Science,* 533, 28–37.

Yeom C. K., S. H. Lee, J. M. Lee, 2000. Study of Transport of Pure and Mixed CO_2/N_2 Gases through Polymeric Membranes, *Journal of Applied Polymer Science,* Vol. 78, 179–189.

Ying Dai, J.R. Johnson, O˘guz Karvan, David S. Sholl, W.J. Koros, 2012. Ultem®/ZIF-8 mixed matrix hollow fiber membranes for CO_2/N_2 separations, Journal of Membrane Science 401– 402, 76– 82.

Zi Tong, Winston Ho, 2017. Facilitated transport membranes for CO_2 separation and capture, Separation Science and Technology, Vol.52, No.2, 156-167.

Zimmerman C.M., Anshu Singh, W.J. Koros, 1997. Tailoring mixed matrix composite membranes for gas separations, *Journal of Membrane Science*, 137, 145-154

http://edgar.jrc.ec.europa.eu/overview.php?v=CO2andGHG1970-2016 accessed on 1.26.2018

http://time.com/4542889/carbon-dioxide-400-ppm-global-warming/ accessed on 1.26.2018.

http://www.power-eng.com/articles/print/volume-120/issue-12/features/petra-nova.html accessed on 2.8.2018

http://www.powermag.com/capturing-carbon-and-seizing-innovation-petra-nova-is-powers-plant-of-the-year/?pagenum=5 accessed on 2.8.2018

https://en.wikipedia.org/wiki/Nitrogen#Gas accessed on 1.26. 2018

https://industry.airliquide.us/carbon-dioxide accessed on 1.26. 2018

https://www.co2.earth/accessed on 10.2.2017

https://www.eia.gov/todayinenergy/detail.php?id=33552 accessed on 2.1.2018

https://www.epa.gov/ghgemissions/overview-greenhouse-gasesaccessed on 1.26.2018

****